WYLE LABORATORIES
SCIENTIFIC SERVICES AND SYSTEMS GROUP
EASTERN OPERATIONS
FACILITIES LOCATED IN
HUNTSVILLE, ALA. AND HAMPTON, VA.

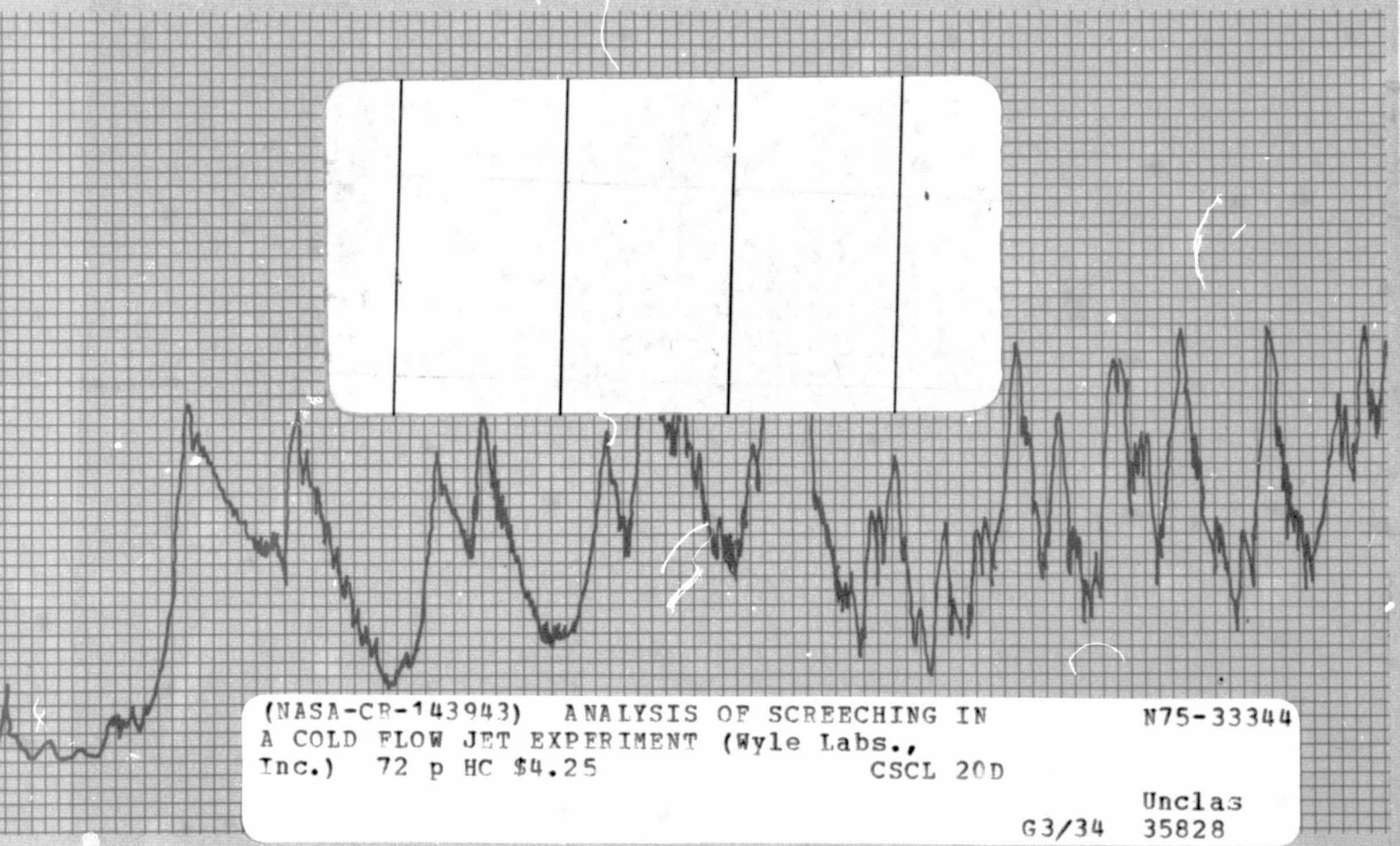

research REPORT

WYLE LABORATORIES — RESEARCH STAFF
REPORT WR 75-2

ANALYSIS OF SCREECHING IN A COLD FLOW JET EXPERIMENT

By

M. E. Wang
R. M. Slone, Jr.
J. E. Robertson
L. Keefe

Work Performed Under NASA-MSFC Contract No. NAS8-30747

June 1975

WYLE LABORATORIES

Copy Number:

SUMMARY

The screech phenomenon observed in a 1/60 scale model Space Shuttle test of the Solid Rocket Booster exhaust flow noise conducted by NASA-MSFC has been investigated. A critical review is given to the cold flow test data representative of Space Shuttle launch configurations to define those parameters which contribute to screech generation. An acoustic feedback mechanism is found to be responsible for the generation of screech. A simple equation which permits prediction of screech frequency in terms of basic testing parameters such as the jet exhaust Mach number and the separating distance from nozzle exit to the surface of model launch pad is presented and is found in good agreement with the test data. Finally, techniques are recommended to eliminate or reduce the screech.

TABLE OF CONTENTS

LIST OF FIGURES

LIST OF FIGURES (CONTINUED)

LIST OF SYMBOLS

c	speed of sound
d	$d = h + L_s$
D	diameter of model SRB nozzle exit
f	frequency in hertz
h	distance from the nozzle exit to the surface of the launch pad
ℓ	distance from the "neck" of an overexpanded jet to the nozzle exit
L_s	distance from separation point on the nozzle wall to the nozzle exit
M_j	jet Mach number
OASPL	overall sound pressure level
OBSPL	octave bandwidth sound pressure level
1/3 OBSLP	one-third octave bandwidth sound pressure level
P	reservoir pressure
P_0	atmosphere pressure
P_s	jet flow separation pressure
R	Reynolds number
S	Strouhal number
SPL	sound pressure level in dB
SRB	Space Shuttle Solid Rocket Booster
V_c	ring vortex convection velocity
V_j	jet exit velocity
α	semi-angle of nozzle divergence
θ	angle between the jet axis and the normal of the obstructing surface

1.0 INTRODUCTION

The propulsion system of the Space Shuttle will create an intense acoustic pressure environment over the external surfaces of the vehicle. This environment will be particularly severe during the early stages of liftoff due to the interaction of the rocket exhaust flow with the launch pad. Definition of the launch acoustic environment of the Space Shuttle is required to ensure its overall structural integrity, reliability, and economical operational requirements. Accurate definition of this environment is necessary at the earliest possible time during the development of the Space Shuttle.

To facilitate a preliminary definition of the Space Shuttle rocket noise environment during liftoff, a series of parametric tests were conducted at the NASA-Marshall Space Flight Center using cold flow jets. These tests were performed with 1/60-scale cold flow nozzles simulating the scaled weight flow of the Shuttle SRBs. The primary objective of these tests was to determine the resultant trends on the Space Shuttle acoustic environment due to liftoff and drift of the vehicle relative to several simulated launch pad configurations. During the course of these experiments, a discrete tone or "screech" was observed in the radiated noise field of the jet. This screech was observed to be highly dependent on the orientation of the Shuttle model relative to the simulated launch pad. Understanding the observed phenomena is considered to be important in order to ascertain if this screech is an anomaly associated only with the cold flow test or if it is indeed associated with the full-scale Space Shuttle launch configuration as well.

The primary objective of this research program is to perform a critical examination of the "screech phenomena" which has been observed and to develop an analytical model which clearly relates the source mechanism to the radiated noise. Finally, an evaluation of the model test data is made with regard to its application to full-scale Shuttle launch configurations. From these results, a test program can be specified and conducted to provide methods of eliminating or suppressing the discrete frequency noise.

It has been determined that the screech noise observed in the cold flow test is associated with a self-exciting acoustic feedback mechanism resulting from the interaction between the model launch pad and the jet flow impinging upon the launch pad. This acoustic feedback mechanism, which was first investigated by Wagner [32] and later extended by Neuwerth [33, 34] in their experimental studies of acoustic radiation due to jet impingement on an obstacle, explains the major features of the subject test data. An equation proposed by Neuwerth to correlate the basic flow parameters to the screech was used to compute the frequencies of the screech modes. The results are found in good agreement with the cold flow test data.

In this report discussions regarding the interpretation of test data and the basic screech-generating mechanism are presented. In the final section conclusions and recommendations on possible methods to either reduce or eliminate the screech are provided.

2.0 DESCRIPTION OF EXPERIMENT

The primary objective of the cold flow test was to define the trend of the Space Shuttle acoustic environments due to liftoff and drift of the vehicle relative to simulated launch pads with different exhaust hole configurations. Two 1/60-scale cold flow nozzles simulating the scaled weight flow of the Shuttle SRBs were used to perform the test.

The arrangement of model test apparatus for the cold flow jet noise experiment is shown in Figure 1. The models consisted of two nozzles which exhausted parallel cold jets through rectangular openings in a simulated launch pad. The Space Shuttle model was held stationary on a fixed-frame structure and the launch pad was mounted on a movable platform which permitted the launch pad assembly to be moved either vertically or horizontally, allowing acoustic measurements for various nozzle-to-pad distances and selected drift distances. The sound pressure levels resulting from the interaction between jet exhaust and the model launch pads were recorded by a set of six microphones located as shown in Figure 1. The geometry of the various launch pad configurations used in the test is shown in Figure 2. The details of the cold flow test can be found in Reference 1.

3.0 EXPERIMENTAL EVIDENCE OF SCREECH

3.1 Presentation of Test Data

It is apparent that a narrow band screech is present in some of the subject cold flow acoustic test data. In order to demonstrate the effect of changing the launch pad configuration and of changing the distance from the nozzle exit to launch pad surface on the screech phenomenon, the test data are presented in the following way: Figures 3 through 8 depict the effect of changing exhaust hole geometry on the measured sound pressure level spectrum for h/D = 0, 1, 2, 4, 8, and 16 respectively; the decimal designation (i.e., .1, .2, etc.) indicates the number of the transducer location depicted in a given figure.

3.2 Observations on the Test Data

The presence of a discrete tone is strongly indicated in much of the 1/3 OBSPL data. However, standard one-third octave band analysis does not always clearly identify the presence of screech; any discrete frequency content is indicated at least one-third octave in bandwidth. Nevertheless, the following trends are discernable:

- For a normalized nozzle exit axial height of h/D = 0, corresponding to the case when the nozzle exit is in the plane of the launch pad surface, measured noise is generally broadband in nature with the effect of launch pad hole size on measured noise showing the following trend:

$$\text{SPL}\left[\begin{matrix}\text{Reduced}\\ \text{Hole Size}\end{matrix}\right] < \text{SPL}\left[\begin{matrix}\text{Nominal}\\ \text{Hole Size}\end{matrix}\right] \leq \text{SPL}\left[\begin{matrix}\text{Widened}\\ \text{Hole Size}\end{matrix}\right] \leq \text{SPL}\left[\begin{matrix}\text{One Large}\\ \text{SRB Hole}\end{matrix}\right]$$

  More specifically speaking, while the SPL spectra obtained for launch pads with larger exhaust holes are nearly identical to one another over the bandwidth of interest, those obtained for a launch pad with reduced size holes display a unique character with lower sound pressure levels.

  A second important observation in the h/D = 0 data is the possible presence of discrete tones as indicated by microphones number 3, number 4, and number 6, as shown in Figures 3.3 and 3.4 (the spectrum taken by microphone number 6 is not shown). Although one-third octave band analysis does not always permit the identification of discrete tone contents, the implication of the test data is that a discrete tone may be present in the one-third octave bands centered at 1,000 Hz and 1,600 Hz.

- At h/D = 1 and h/D = 1.5 the one-third octave band spectra of the measured data follow the same basic trends as observed in the data for h/D = 0, except that the variation of the launch pad hole size shows a slightly lesser effect on the sound pressure level.

- At h/D = 2 the one-third octave band SPL spectra for the various launch pad configurations are generally similar to one another with the exception that discrete tone peaks were evident for those pad configurations with reduced hole size and with nominal hole size. This is clearly shown in Figures 5.1 through 5.4.

- At h/D = 4 the variation in 1/3 OBSPL with variation in launch pad exhaust hole size demonstrates an entirely different character from the previous cases. Generally,

$$\text{SPL}\begin{bmatrix}\text{Reduced}\\ \text{Hole Size}\end{bmatrix} > \text{SPL}\begin{bmatrix}\text{Nominal}\\ \text{Hole Size}\end{bmatrix} > \text{SPL}\begin{bmatrix}\text{Widened}\\ \text{Hole Size}\end{bmatrix} > \text{SPL}\begin{bmatrix}\text{One Large}\\ \text{SRB Hole}\end{bmatrix}$$

  Of particular significance in the h/D = 4 1/3 OBSPL data is that screech appears to be extremely strong as indicated by the high sound pressure levels of one-third octave bands centered at 1,000 Hz and 1,600 Hz, and at frequencies between 4,000 Hz and 5,000 Hz. Furthermore, it is clearly indicated in the data (Figures 6.1 through 6.4) that the spectrum shape is influenced by variation of the launch pad jet exhaust hole size, which implies that the size of the exhaust hole could be an important factor affecting the screech-generating mechanism.

- At h/D = 8 narrow-band screech is evident in one-third octave bands centered at 1,000 Hz and 2,000 Hz. The data are ordered in such a way that an increase in launch pad jet exhaust hole size is accompanied by a decrease in overall sound pressure levels, i.e.,

$$\text{SPL}\begin{bmatrix}\text{Reduced}\\ \text{Hole Size}\end{bmatrix} > \text{SPL}\begin{bmatrix}\text{Nominal}\\ \text{Hole Size}\end{bmatrix} > \text{SPL}\begin{bmatrix}\text{Widened}\\ \text{Hole Size}\end{bmatrix} > \text{SPL}\begin{bmatrix}\text{One Large}\\ \text{SRB Hole}\end{bmatrix}$$

  It is of interest to note that the 1/3 OBSPL components at frequencies above 3,150 Hz are rather insensitive to change in launch exhaust hole size.

- At h/D = 16 the sound pressure level spectra exhibit a trend similar to the h/D = 8 case for change in launch pad exhaust hole size, except that no narrow-band screech is apparent. Also, the 1/3 OBSPL components are less sensitive to the change in launch pad configurations.

In addition to the above observations, several key features of the test data are noted:

a) Although narrow-band peaks appear to be present for h/D = 0 and h/D = 1, it should be noted that, unlike the cases of h/D = 2, 4, 6, where similar peaks were recorded by all six microphones, only microphone numbers 3 and 6 indicated the presence of screech. An inspection

of the location of microphones number 3 and number 6 suggests that acoustic reflections off a nearby pipe flange near microphones number 3 and number 6 might explain this anomaly.

b) At $h/D = 4$ and $h/D = 8$ the strength of the narrow-band screech components decreases with increasing exhaust hole sizes and apparently diminishes to a state where no appreciable peaks are presented.

c) The 1/3 OBSPL spectrum for a free jet which is clearly over-expanded, does not show any apparent evidence of discrete peaks that normally are associated with an imperfectly expanded supersonic jet.

The above observations suggest that mechanisms other than eddy-shock interaction may play the predominant role in the generation of discrete tones.

Examination of the experimental setup of the MSFC cold flow test reveals a similarity to a jet-orifice interaction experiment where discrete tones of a pattern similar were observed. This suggests that the mechanism which gives rise to a discrete tone in the case of jet-orifice interactions may be responsible for the screech observed in the Space Shuttle launch simulation test.

In the next section the discrete tone generation mechanism in jet-orifice interaction, as well as its applicability to the MSFC launch simulation cold flow test, is examined in detail.

4.0 BASIC SCREECH-GENERATING MECHANISMS

4.1 Review of Previous Work

It was observed in previous sections that there is a close analogy between the experimental setup of the subject cold flow tests and the devices through which a "hole tone" was observed in previous tests. In order to gain insight into the screech noise-generating mechanism it is worthwhile to discuss the hole tone and related phenomena.

It is known that the hole tone is due to jet-orifice interactions. When an air jet is exhausted through an orifice with a sharp edge, a feedback mechanism which gives rise to discrete tones is sometimes established.

The phenomenon of the hole tone has received the attention of scientists since 1854 when Sandhaus [40] published a paper to discuss the mechanism of a whistling teapot. The teapot whistling device consists of two concentric orifices a short distance apart. When the water inside the teapot boils, large amounts of vapor are blown through the first orifice, resulting in a vapor jet which, when it interferes with the second orifice, gives rise to a whistle. He found that the tone frequencies, f, are related to jet speed, U, the separation distance between the two orifices, h, and the orifice diameters, D, by $f \sim F(D/h) \cdot U/h$ where $F(D/h)$ is an undetermined function of D/h.

Rayleigh [40, 42] later discussed this phenomenon in his study of "bird calls" which, in principle, are also hole tones. In an effort to explain the generation of the bird call, he proposed the following mechanism: A disturbance of the bird's exhaled breath at a downstream orifice is transmitted upstream at the speed of sound to the first plate where it interacts with the jet and yields further disturbances which are amplified by the disturbed jet as they are convected downstream and an acoustic feedback loop is established. He concluded that, in the hole tone phenomenon, the Strouhal number, S, is a function only of Reynolds number, R, and the normalized orifice separating distance, h/D, i.e.,

where:

$$S = S(R, h/D)$$

$$S = f \cdot D/U$$

$$R = U D/\upsilon$$

f = hole tone frequency

D = orifice diameter

h = orifice separation distance

υ = kinematic coefficient of viscosity

Since Rayleigh's study there have been a number of studies on this topic, among which the better known are those of Von Gierke [47], Anderson [41], Chanaud and Powell [42], Becker and Massaro [39], and Wilson et al [44].

In a series of experimental investigations on pipe tones, Anderson [41], using a shadowgraph technique, evidenced a periodic shedding of ring vortices from the edge of an orifice in an airstream. The downstream ring vortex expands and slows down while the upstream ring vortex contracts, speeds up, and finally coalesces with the preceding downstream vortex.

In 1952 Von Gierke conducted experiments on hole tones due to interaction between a jet and an orifice when the jet was exhausted through the orifice, but he did not relate the discrete tone to an acoustic feedback mechanism such as previously described.

Chanaud and Powell [42] performed experiments in 1964 to extend Von Gierke's study of hole tones. They found that discrete tones can be generated when objects obstruct the path of an axisymmetric jet. In their experimental study, a plate with a circular hole of the same size as the jet diameter at the nozzle exit was placed at various distances downstream of the nozzle exit and discrete tones were detected for certain nozzle-to-plate distances. An acoustic feedback mechanism similar to the one proposed by Rayleigh was believed to yield discrete tones. It was also indicated that the axisymmetric jet system is sensitive to reflected acoustic waves, even those which are relatively weak.

The experimental setup with which Chanaud and Powell studied the hole tone is shown in Figure 9 in comparison with the schematic diagram showing the subject cold flow test setup. In a later paper Chanaud further classified the aerodynamic whistle into three different types according to the mechanism through which the feedback of energy excites the instability of the jet flow.

A block diagram which represents such a classification system is given in Figure 10, from which it can be seen that the class I feedback mechanism is likely to occur for the setup shown in Figure 9.

In 1967 Becker and Massaro [39] studied the acoustic sensitivity of jets. They found that for several types of acoustic excitation, including pure tones, a ring vortex was observed to roll up in the jet boundary layer, then coalesce with preceding vortex rings and eventually disintegrate into turbulent eddies.

More recently the understanding of tone-generating mechanisms was significantly advanced by Wagner and Neuwerth [32, 33, 34]. Their work provides a credible explanation of the screech apparent in the MSFC cold flow test data.

In his investigation of the sound field resulting from the impingement of an axisymmetric, high speed, subsonic air jet on a wall, Wagner [32] observed a standing wave pattern in the jet core, the convection of ring vortices downstream in the jet boundary layer, and a pronounced discrete tone of high intensity in the SPL spectra. Wagner explained his observations in the following way (similar to the feedback mechanism as described by Chanaud): The boundary layer of the jet is very sensitive to periodic disturbances. In the jet boundary layer near the nozzle exit ring vortices are evolved periodically, which are convected downstream distances on order of magnitude of nozzle diameter while gathering strength and becoming larger in size. When the ring vortex strikes on an obstructing surface a

pressure pulse or disturbance is emitted which propagates upstream—in part externally to the jet flow in the form of sound wave and in part internally to the free-shear layer—and excites the evolution of a new ring vortex. Thus an acoustic feedback loop is established.

Obviously, both the acoustic wave and the pressure pulse travelling upstream must arrive at the origin of the jet boundary layer at the right moment in order to excite the shedding of a ring vortex, and hence to maintain the feedback loop. Since, for a given distance from the nozzle exit to launch pad, this requirement is fulfilled only by those acoustic waves of a particular wavelength, the mechanism thus supports discrete tones.

Neuwerth [33, 34] extended Wagner's study to the case of under-expanded supersonic jets, which is different from subsonic impingement in that discrete frequency acoustic radiations may occur even without the introduction of an obstructing surface. In this case, i.e., $M > 1$, the backward moving pressure pulse can no longer propagate upstream inside the jet with the speed of sound. The free-shear layer is disturbed by the obstructing surface, creating an acoustic wave which propagates upstream via a path external to the jet flow. This acoustic wave reaches the origin of the free-shear layer and excites the shedding of a ring vortex girdling the jet flow. The ring vortex travels down the jet, impinges upon the obstruction, and a subsequent acoustic wave is propagated back upstream. From that point, the process repeats with a period determined by the distance of the obstruction from the origin of the free-shear layer and the velocity of the jet.

In addition to a general discussion of this mechanism, Neuwerth mentioned several particulars derived from his experimental work. He noted for the under-expanded supersonic jet that even when Powell's feedback mechanism is present in the free jet, his proposed mechanism dominates when impingement occurs.

Also the feedback loop breaks down for obstruction distances greater than $h/D = 7$ (for an under-expanded jet). The explanation of this feature lies in the fact that a ring vortex has a finite lifetime as it is convected downstream. Even though it is growing in strength, it is also being subjected to heavy energy dissipation due to momentum exchange with the static ambients and other disturbances in the shear layer. Thus an obstruction placed beyond some maximum "vortex lifetime" distance will not be struck by a discrete ring vortex, but rather by uncorrelated eddies—the fragments of a destroyed ring. The resulting pressure pulse emitted from these eddies will remain uncorrelated with each other as they propagate back to the origin of the shear layer. Such random excitation of the shear layer does not give rise to the shedding of ring vortices as a correlated stimulus would. Additional experimental work by Neuwerth [34] implies that the ring vortex does not have to be entirely obstructed circumferentially in order that feedback may occur. A final point noted by Neuwerth's experiment is the destruction of feedback by inclining the obstructing surface. Neuwerth found no feedback for a surface inclination angle with respect to the jet axis of less than 35 to 40 degrees.

Convincing confirmation of Neuwerth's theories are found in the Schlieren photographs in his report. Of particular interest is the case of the supersonic jet displayed in his Figure 18 (schematically depicted in Figure 9) where the ring vortices can be seen being convected along the boundary layer of the jet towards the plate and the acoustic wavefront is visible propagating in the opposite direction.

4.2 Application of Acoustic Feedback Model to MSFC Cold Flow Scale-model Test

From prior discussion, the applicability of a "hole tone model" or a "jet impingement model" to the MSFC cold flow test data is self-evident. As was mentioned earlier, the experimental setup of the MSFC cold flow test was physically similar to those of the hole tone experiments and of the jet impingement on an obstruction previously performed by others. The screech tone does not appear until the separation distance from the nozzle exit to the model launch pad falls into the interval where the hole tone or jet impingement tone occurs. Further experimental evidence to support this view comes from the MSFC cold flow test, where the acoustic characteristics due to impingement of a model SRB jet on a model launch pad without an exhaust hole (i.e., a flat plate) was investigated. Figures 11.1 through 13.6 show the 1/3 OBSPL spectra for the cases $h/D = 4$, 8, and 16 compared to those for model launch pads with reduced-size hole and with one large exhaust hole under the same testing conditions.

It is apparent from each of these diagrams that the 1/3 OBSPL spectra corresponding to the case of jet impingement on a flate plate essentially envelop those curves obtained for the cases in which the model pads have exhaust holes. And, in particular, the location of frequency peaks in each of those cases agree with one another almost perfectly.

These facts clearly imply two important conclusions: Firstly, it can be concluded with more confidence that the acoustic feedback mechanism which yields discrete tones observed in hole tone experiments and in experiments of jet impingement on obstructions is the one responsible for the screech phenomena observed in the MSFC launch simulation cold flow test. Secondly, in order to cause screech it is not necessary to obstruct the jet flow or the ring vortices peripherally; even a partial obstruction of the ring vortices is enough to cause the feedback mechanism, and thus the screech, to occur.

In order to show how the cold flow test data fits into the physical model proposed by Wagner and Neuwerth, a more precise determination of the size of the jet relative to the size of the exhaust hole in the model launch pad is required.

Since the model SRB nozzles are designed to permit perfect expansion at $M = 3.72$ against a back pressure of 2.1 psia (see Table I), the jet must be highly over-expanded under the flow conditions at which the MSFC cold flow test was performed. In this case, the jet flow separates from the nozzle wall [24, 26, 31], and the effective jet exit diameter at the separation point is thus less than the actual nozzle exit diameter.

Experiments [24-26, 31] with over-expanded rocket nozzles indicate that separation will occur where the jet static pressure is approximately 0.37 to 0.41 of the exit back pressure. The exact values of separation pressure is influenced by the character of the boundary layer and the semiangle of the nozzle divergence, α. However, reported experiments showed that for a given α, the separation pressure is a function of reservoir pressure, as shown in Figure A.1 in Appendix A [24]. As a first approximation, it is acceptable to take $P_s = 0.4\ P_0$

TABLE I.
COMPARISON OF FULL-SCALE AND MODEL NOZZLES*

PARAMETER (Units)	FULL-SCALE SRB	MODEL SRB
D_e (in.)	141.7	2.498
D_t (in.)	54.2	0.866
A_e/A_t	7	8.32
γ	1.18	1.4
$M_{e_{vac}}$	3.0	3.72
$V_{e_{vac}}$ (ft/sec)	7,900.	2,200.
T_o (°R)	6,125.	530.
$T_{e_{vac}}$ (°R)	3,403.	140.6
P_c (psia)	747.	218.
$P_{e_{vac}}$ (psia)	15.	2.1
$\dot{w}$ (lbm/sec)	10,715.	2.98
T_{vac} (lb)	2.856×10^6	213.8

*These calculations are based on vacuum flow conditions.

(where P_s = separation pressure and P_0 = the atmospheric pressure) to calculate the nozzle exit parameters. It is obtained by calculations given in Appendix A that

$$\frac{A_s}{A_t} = \frac{A_s}{A^*} = 4.35 , \qquad A_t = 0.866 \text{ in.}$$

$$\frac{D_s}{D_t} = 2.09$$

$$M = 3.01$$

$$V_j = 2183 \text{ ft/sec} = 666 \text{ m/sec}$$

$$D_s = 1.835 \text{ in.}$$

$$L_s \simeq 1.3 \approx 1.375 \text{ in.}$$

Note that the jet diameter at the separation point is 1.835 inch rather than 2.5 inches.

Notice should also be given to the fact that flow separation in an over-expanded jet is always accompanied by an oblique shock wave and reduction in the jet size so that the pressure in the jet flow can approach atmospheric pressure. The minimum size of a separated, over-expanded jet usually lies from 0.5 to 1.5 effective nozzle diameters downstream of the separation point, dependent upon the reservoir pressure. In Figure 14 the normalized distance from the point of minimum jet diameter to nozzle exit is plotted against the ratio of tank pressure to ambient pressure based on shadowgraph in reference 35 for a nozzle designed for M = 1.92. The extrapolation of the curve shows that for large pressure ratio the normalized distance from jet minimum to nozzle exit approaches 1.5 asymptotically. Although, at this point, it may be unrealistic to employ this value for the model SRB nozzles which are designed to permit full expansion at M = 3.72, comparison with the result of other experiments [14, 27, 31] and theoretical prediction [19] suggests that this value may be a good approximation.

It is possible, based on the above considerations, to determine how the jet exhaust is obstructed by portions of the model launch pad.

Previous experimental workers [21, 27, 38] have found that the boundaries of off-design supersonic jets expand at an angle from 10 to 15 degrees, or at a rate approximately x/5.67 to x/3.75, where x represents the distance from the nozzle exit. Applying this rate of spread to the calculations reveals that for the subject cold flow tests not until approximately h/D = 2 will the exhaust jet have diverged enough to cause impingement of the jet on the pad surface separating the two reduced size exhaust holes. Figure 15 shows the schematic

diagram of the predicted jet flow onto the model launch pad two exit diameters downstream of the nozzle exit. It can be seen from this picture that h/D = 2 is the minimum limiting, separating distance for which impingement of ring vortices takes place. It is therefore anticipated that the acoustic feedback, as described in preceding sections, does not occur until the model nozzle is at some height at least two nozzle diameters above the pad (with reduced hole size).

As the rocket nozzle rises further above the pad more of the convecting ring vortices strike the pad surface and one might expect the pressure disturbances to be stronger. Similarly, for a given separation, more of the ring vortices will be struck by a launch pad with small holes (larger center strip) rather than one with large holes (smaller center strip). The trends so described are reflected in the measured data.

4.3 Influential Factors to Screech Generation

Since one of the objectives of this study is to assess the screech observed in the cold flow scale-model test for the full-scale Shuttle launch configuration, the effects of temperature and scaling, which represent the key differences between the scale-model test and the full-scale launch, are addressed.

An experiment performed by Neuwerth [34] using a hot jet at a temperature of 500°K has shown that the strength of screech is weakened due to increase in jet temperature. This effect suggests that during the launch of the full-scale Space Shuttle the screech might be diminished by the extremely high temperatures. However, the ultimate effect of temperature and its potential to eliminate the screech will have to be determined.

The scaling is known to affect the screech frequency in such a way that for a fixed jet exit Mach number and nozzle-to-pad spacing the nozzle, a larger exit diameter tends to generate a screech of lower frequency. This can be expressed by the following relation:

$$f_1 / f_2 = D_2 / D_1 , \qquad M_j = \text{const. and } h/D = \text{const.}$$

It is therefore anticipated that, should there be any screech present during the launch of full-scale Shuttle, it will be at a low frequency.

To explain the reduced screech strength for the h = 8D case and the disappearance of screech completely for h = 16D, it is well to remember that a vortex ring has a finite lifetime. As vortex rings are convected downstream they are dissipated by the turbulence of the flow and tranquil air outside the flow until the ring vortices disintegrate and become piecewise eddies.

No known experiment has investigated the vortex lifetime for over-expanded jet at a velocity comparable to that of the MSFC cold flow test (M = 3.01). It was reported by Crow and Champagne [45] in their investigation of the "orderly structure" in a low speed subsonic jet ($R < 3 \times 10^5$) that such vortex structure does not last beyond h/D = 6. Wagner showed [32]

that for impingement of a jet having an exit velocity in the range of $0.75 \leq M \leq 0.95$, no discrete tone was detected for separation distances beyond five nozzle diameters. In a similar experiment by Olsen et al [46], screech in a one-third octave band centered at 2000 Hz was observed for a subsonic jet with $M_j = 0.85$ ($V_j = 293$ m/sec) at separating distances of 4.7 D and 7.05 D where D is the jet nozzle exit diameter.

Neuwerth's investigation of the impingement of an under-expanded supersonic jet has shown that the ring vortices prevail up to seven nozzle diameters downstream of the nozzle exit before disintegration.

If consideration is given to the fact that starting from the jet minimum, which is approximately 1 D to 1.5 D from the nozzle exit, the shock structure in an over-expanded jet is quite similar to that of an under-expanded jet, then it may be possible that a separating distance of 7 D for an under-expanded jet could actually be 8 D or more for an over-expanded jet. No flow visualization investigation has been identified in the published literature for an overexpanded jet with a flow velocity comparable to the MSFC cold flow test. Since the cold flow test data for $h/D = 8$ showed distinct peaks in a one-third octave band centered at 1000 and 2000 Hz, it is believed that ring vortex impingement on launch pad surface and hence the acoustic feedback mechanism did occur for the $h/D = 8$ case in the MSFC cold flow test.

5.0 MATHEMATICAL MODEL

It has been concluded in the previous section that the acoustic feedback mechanism as described by Neuwerth is responsible for the screech generation in the MSFC cold flow scale-model test.

The general agreement between the cold flow test data with Neuwerth's test results suggests that the semiempirical formula developed by Neuwerth to predict the screech frequency based on testing parameters may be applicable to the subject cold flow tests.

Neuwerth gave the following formula (Appendix B):

$$f = \frac{n V_c}{d\left(1 + M_c\right)}$$

where f = screech frequency in Hz

n = characteristic integer

V_c = convection velocity of ring vortex

M_c = convection Mach number with respect to atmospheric speed of sound

d = distance from origin of jet-shear layer to surface of launch pad

This equation can be modified in the following way:

$$f = \frac{n \cdot V_j \cdot \left(V_c / V_j\right)}{d\left[1 + \left(V_c / V_j\right)\left(V_j / C\right)\right]}$$

If the ratio of V_c / V_j is taken, in accord with Neuwerth's investigation of subsonic jet with $M_j = 0.95$, to be 0.62 (note that by definition $M_j = V_j / C$), this equation can be expressed as (see Figure 16):

$$f = \frac{n \cdot V_j \cdot (0.62)}{d\left(1 + 0.62\, M_j\right)} = \frac{n \cdot V_j \cdot (0.62)}{\left(h + L_s\right)\left(1 + 0.62\, M_j\right)}$$

where L_s is the distance from the flow separation point to the nozzle exit and h is the distance from the nozzle exit to the launch pad surface. Now that the jet exhaust velocity, V_j, the jet nozzle exit Mach number, M_j, are known, the screech frequency, f, can be calculated for different values of d, the effective nozzle exit to the launch pad surface. The calculated screech frequencies for the various separating distances of h/D = 2, h/D = 4, h/D = 8 are presented in Table 2 for n = 1, 2, 4. Comparison between the predicted frequency and the test data shows that agreement is generally achieved within one-third octave band. At h/D = 2 for n = 2, the calculated frequency is 2086 Hz, which falls within the 2 kHz one-third octave band where a distinct peak was registered in the test data. At h/D = 4 for n = 2, 4, and 8, the computed frequencies are respectively 1035 Hz, 2071 Hz, and 4142 Hz, each of which, again, fall within the one-third octave band where peaks in the data are most prominent. Finally, at h/D = 8 for n = 4, the screech frequency was computed to be f = 1098 Hz, again in agreement with the data. Neuwerth's theory predicts not only the general trend of the measured data but also more specific features. Although the agreement between Neuwerth's model and the MSFC cold flow model test data is not universal, it is felt that the acoustic feedback mechanism proposed by Neuwerth did occur during the subject acoustic tests.

TABLE II.
COMPUTED SCREECH FREQUENCIES

		DISTANCES FROM NOZZLE EXIT TO LAUNCH PAD SURFACE h			
		2 D (5")	4 D (10")	6 D (15")	8 D (20")
SCREECH FREQUENCY IN HERTZ	n = 1	1,043 Hz	502 Hz	347 Hz	266 Hz
	n = 2	2,086 Hz	1,003 Hz	695 Hz	532 Hz
	n = 4	4,172 Hz	2,007 Hz	1,391 Hz	1,064 Hz
	n = 8	8,344 Hz	4,014 Hz	2,783 Hz	2,128 Hz

where: D = SRB's nozzle diameter
n = period numbers

NOTE: The computation based on the equations persented in section 5.0. The underlined numerical values represent those which fit right on the discrete peaks in the subject cold flow test data.

6.0 ELIMINATION OF SCREECH NOISE

Since the acoustic feedback mechanism described in the last section is believed to be responsible for the screech noise observed in the MSFC cold flow test, it is thus apparent that the elimination of screech can be accomplished by either of the following measures:

1) Ensure that all reflecting surfaces in the jet flow are beyond the point downstream where convecting ring vortices dissipate.

2) Destroy the convecting ring vortices before they can impinge on a reflective surface.

The first above is best demonstrated by the case at h/D = 16 in the MSFC cold flow tests, where no apparent screech components was presented. Several tactics based on (2) above may be used to prevent the acoustic feedback loop from becoming fully established and hence to eliminate the screech. For instance, the use of a protuberance at the nozzle exit of the size of the jet boundary layer thickness or a corrugated nozzle lip have proved most effective in suppressing the feedback loop.

The effect of a protuberance at the nozzle exit on the acoustic feedback mechanism was investigated by Neuwerth 33 who inserted a pin into the boundary layer of the jet flow. It was found that the harmonics of the fundamental screech mode disappear when the pin is inserted into the jet flow to a depth of D/100, where D is the diameter of the nozzle exit, and the suppression of the fundamental mode is achieved by an insertion depth of D/20. In fact, with the presence of a protuberance at the nozzle lip, ring vortices were still formed, but they were not closed and evidently disintegrated before arriving at the obstructing surface.

Protuberances of this kind, when located at stations further downstream of the nozzle exit, are less effective since they then become too small compared with the size of the ring vortices to effectively interfere their formation.

Experiments were also conducted by Neuwerth to study the effect on the screech generation of inclining the obstructing surface. He found that no screech was detectable for an angle between the jet axis and the surface of less than 45 degrees. This result is understandable since, firstly, the pressure disturbances generated at the obstructing surface, which, instead of propagating toward the jet nozzle exit and completing the acoustical feedback loop, are reflected in another direction according to the laws of reflection; and, secondly, the velocity component at which the jet or the ring vortex strikes the obstructing surface is reduced resulting in a decrease in the strength of pressure disturbances.

From a practical standpoint, it may not be desirable to modify the interior of the nozzle with protuberances of any kind or to use a nozzle with a corrugated exit since it may result in substantial loss of jet thrust.

Thus, a more practical approach to control full-scale screech noise may lie in judicious design of the launch pad. The launch pad should be designed and located so that the jet does not impinge on a solid reflecting surface until it is beyond the range of the ring vortex's lifetime.

For the MSFC cold flow test set-up, a simple calculation based on the assumption that the jet exhausts at a spreading rate of h/6 and that the ring vortex has a lifetime of 8 D shows that in order to avoid screech, the edge of the exhaust hole should be at least at a distance of δ from the jet axis. Where δ is given as:

$$\delta = \frac{1}{2} D_{eff} \left[1 - \tan(\theta - \alpha)\right] + \frac{1}{6}\left[h - \left(D - L_s\right)\right]$$

for $D_{eff} = 1.835$ inch

$D = 2.5$ inches

$h = 8\,D = 20$ inches

$\theta = 19$ degrees

$\alpha \simeq 12$ degrees at separation point.

It is obtained that $\delta \simeq 4.0$ inches.

This implies that screeching cannot be avoided as long as the launch pad has a solid center piece between two holes since, for all cases, jet impingement occurs within the range of ring vortex lifetime, believed to be about 8 nozzle diameters downstream of the nozzle exit. Naturally screeching is unlikely to occur for a model launch pad with one large exhaust hole whose edges are, according to the above estimation, 4.0 inches or more off the scaled jet axis.

However, it may be possible to use a model launch pad of smaller exhaust hole whose edge consists of surfaces at an angle of 35 degrees or smaller to the jet axis. It is not possible at this stage to provide precise information regarding the optimal plate angle at which the acoustic feedback loop can be completely destroyed. It is believed further study on this aspect will have to be performed in order to define the most desirable inclined plate launch pad configuration.

Nevertheless, the general layout of the above proposed launch pad configuration has the potential to permit a complete elimination of screech and is conceptually depicted in Figure 17.

Another possibility to eliminate the jet screech is to eliminate the solid reflecting surface of the launch pad altogether. Exposed structural members comprising a grid with a large open/closed area ratio might destroy the ring vortices without reflecting significant amounts of acoustic energy to perpetrate the feedback loop.

These and other possible solutions require further study to determine the most effective method to eliminate any full-scale jet screech at a reasonable cost.

7.0 CONCLUDING REMARKS

The following conclusions are based on the preceding considerations:

1) An acoustic feedback mechanism resulting from interaction between the jet flow and the edge of the model launch pad exhaust hole has been identified as responsible for the screech evidenced in the MSFC preliminary Space Shuttle cold flow model test.

2) An equation developed by Neuwerth to predict the frequency of discrete tones resulting from impingement of a subsonic or an under-expanded supersonic jet on a flat surface has been modified to predict the screech frequency observed in the subject cold flow test in which the SRB jet is known to be heavily over-expanded. Comparison of the prediction with the one-third octave band test data shows that the predicted frequency falls within the one-third octave band where the discrete peaks are most prominent.

3) The similarity between the 1/3 OBSPL spectra obtained for the case of a launch pad without exhaust holes (i.e., flat plate) and those for reduced size holes and one large hole, not only confirms the applicability of acoustic feedback model to the cold flow test data, but also confirms the correctness of previous investigators' finding of the shedding and rolling up or ring vortices along the boundary of the jet exhaust. It is also implied that, in order to produce screech, the jet does not have to strike the edge of the launch pad hole circumferentially.

4) High temperatures tend to weaken the screech. However, the ultimate effect of high temperature and its potential to eliminate the screech will have to be determined by further study. Scaling is known to affect the screech frequency in such a way that, for a fixed jet exit Mach number and nozzle-to-pad spacing, the nozzle with larger exit diameter tends to yield screech of lower frequency according to conventional Strouhal scaling.

5) Complete elimination of screech in cold flow tests is possible by preventing the acoustic feedback loop from being established. This can be accomplished by any one of the following techniques:

   - Utilize a launch pad with a large enough exhaust hole (such as the one presented in section 6.0) so that the interactions between the jet and the launch pad does not occur until it is beyond the ring vortex lifetime.

   - Employ a launch pad with relatively smaller exhaust holes whose edges consist of surfaces at an angle of less than 35 degrees with the jet axis.

- Modify the nozzle interior with protuberances of suitable size to destroy the acoustic feedback loop by breaking up the ring vortex structure before it arrives at the surface of the launch pad.

- Lift the launching position to beyond eight SRB nozzle diameters above the pad so that the ring vortices do not survive the distance.

Of the above techniques all of which are known to reduce or to eliminate the screech noise, only the second is advocated since it permits not only a more flexible design of the launch system but also requires a minimum amount of modification of the whole system without incurring the penalty of lost rocket thrust. However, it is premature at this stage to specify further details regarding the layout of the proposed launch pad system since information on this aspect is still lacking and further study will be necessary.

REFERENCES

1. Northrop Service, Inc., "Space Shuttle Lift-Off Acoustic Analysis Report — Cold Flow Test Series I," M-230-1294, 1974.

2. Powell, Allan, "The Reduction of Choked Jet Noise," Proc. Phys. Soc. B67, pp. 313-327, 1953.

3. Powell, Allan, "Pn the Mechanism of Choked Jet Noise," Proc. of Phy. Soc. B66, pp. 1039-1056, 1953.

4. Powell, Allan, "The Noise of Choked Jets," J. of Acous. Soc. of Amer., Vol. 25, No. 3, pp. 385-389, 1953.

5. Powell, Allan, "On the Noise Emanating from a Two-Dimensional Jet Above the Critical Pressure," Aeron. Quar., Vol. IV, Feb. 1953.

6. Liepmann, H. W., and A. Roshko, Element of Gasdynamics, John Wiley and Sons, Inc., New York, 1957.

7. Zucrow, M. J., Aircraft and Missile Propulsion, Vol I, Chapter 4, pp. 337-378, 1959.

8. Lassiter, L. W., and H. H. Hubbard, "The Near Noise Field of Static Jets and Some Model Studies of Devices for Noise Reduction," NACA Report 1261, 1954.

9. Simcox, C. D., "Effect of Temperature and Shock Structure on Choked Jet Noise Characteristics, AIAA Paper 71-582.

10. Davies, M. G., and D. E. Oldfield, "Tones from a Choked Axisymmetric Jet, Part I. Cell Structure, Eddy Velocity and Source Locations; Part II. The Self-Excited Loop and Mode of Oscillation;" Acustica, Vol. 12, No. 4, 1962.

11. Davies, M. G., "A Note on the Radiation and Cell Pattern of Choked Jets," J. Sound Vib., I(3), pp. 298-301, 1964.

12. Glass, D. R., "The Effect of Acoustic Feedback on the Spread and Decay of Supersonic Jets," AIAA Paper No. 68-81. Also, AIAA Journal, Vol. 6, No. 10, pp. 1890-1897, 1968.

13. Hay, J. A., and E. G. Rose, "In-flight Shock Cell Noise, J. Sound Vib., 11(4), pp. 411-420, 1970.

14. Franklin, R. E., "Noise Measurements on Cold Jets Using Convergent-Divergent Nozzles," Aeron. Quar., Vol. VIII, No. 11, 1957.

REFERENCES (Continued)

15. Westley, R., and J. H. Woolley, "An Investigation of the Near Noise Fields of a Choked Axisymmetric Air Jet," NRC Report LR-506.

16. Lee, B. H. K., and R. Westley, "Effective Source Distribution in a Choked Screech Jet," NRC Report LR-548.

17. Dosanjh, D. S., and F. J. Montegani, "Reduction of Noise from Underexpanded Axisymmetric Jet Flow Impingement," AIAA Paper 68-80.

18. Chan, Y. Y., "A Simple Model of Shock Cell Noise Generation and Its Reduction," NRC Report LR-564, 1973.

19. Chow, W. L., and I. S. Chang, "Mach Reflection from Overexpanded Nozzle Flows," AIAA Journal, Vol. 10, No. 9, 1972.

20. Ollerhead, J. B., "Some Shadowgraph Experiments with a Cold, Supersonic Jet," Wyle Laboratories Research Staff Report WR 66-44, 1966.

21. Ollerhead, J. B., "On the Prediction of the Near Field Noise of Supersonic Jets," Wyle Laboratories Research Staff Report WR 66-45 or NASA CR-857, 1966.

22. Curle, N., "The Influence of Solid Boundaries Upon Aerodynamic Sound," Proc. Roy. Soc., A 216, p. 412, 1953.

23. Karamcheti, K., et al, "Some Features of An Edge Tone Flow Field," NASA SP-207.

24. Green, L., "Flow Separation in Rocket Nozzle," J. ARS, p. 34, Jan-Feb. 1953.

25. Scheller, K., and J. A. Bierlein, "Some Experiments on Flow Separation in Rocket Nozzle," J. ARS, p. 28, Jan-Feb. 1953.

26. Summerfield, M., C. R. Foster, and W. G. Swan, "Flow Separation in Overexpanded Supersonic Exhausted Nozzles," Jet Propulsion, p. 319, Sept-Oct. 1954.

27. Love, E. S., C. E. Grigsby, L. S. Lee, and M. J. Woodling, "Experimental and Theoretical Studies of Axisymmetric Free Jets," NACA TR R-6, 1959.

28. Pack, D. C., "A Note on Prandtl's Formula for the Wavelength of a Supersonic Gas Jet," Quar. J. Mech. and App. Math., Vol. III, Pt. 2, 1950.

29. Morse, P., and Uno Ingard, Theoretical Acoustics, McGraw Hill, 1968.

30. Potter, R. C., "An Investigation to Locate Acoustic Sources in a High Speed Exhausted Stream," Wyle Laboratories Research Staff Report WR 68-4, 1968.

31. "Handbook of Supersonic Aerodynamics," Section 17, NAVWEP Report 1488 (Vol. 6), 1964.

32. Wagner, F.R., "The Sound and Flow Field of an Axially Symmetric Free Jet on Impact on a Wall," NAS TT-F-13942.

33. Neuwerth, G., "Acoustic Feedback of a Subsonic and Supersonic Free Jet Which Impinges on an Obstacle," Royal Aircraft Establishment, Library Translation No. 1739, 1972.

34. Neuwerth, G., "Acoustic Feedback Phenomena of the Subsonic and Supersonic Free Jet Impinging on a Foreign Body," NASA TT-F-15719.

35. Ferri, A., Elements of Aerodynamics of Supersonic Flows, McMillian, 1949.

36. Shapiro, A., "The Dynamics and Thermodynamics of Compressible Fluid Flows," Renald, N.Y. (1953).

37. Richards, E. J., and D. J. Mead, Noise and Acoustic Fatigue in Aeronautics, John Wiley, 1968.

38. Pei, S.I., Fluid Dynamics of Jets, Van Norstrand, 1954.

39. Becker, H.A., and T. A. Massaro, "Vortex Evolution in a Round Jet," J. Fluid Mech., Vol. 31, Pt. 3, 1968.

40. Rayleigh, J. W. S., Theory of Sound, Dover, Vol. 2, pp 410-414.

41. Anderson, A.B.C., "Pipe Tone," JASA, Vol. 24, No. 6, pp 675-681 (1952), JASA, Vol. 25, No. 4, pp 626-631 (1953), JASA, Vol. 27, No. 6, pp 1048-1053 (1955).

42. Chanaud, R. C., "Some Experiment Concerning the Hole and Ring Tone," JASA, Vol. 37, No. 5 (1965).

43. Chanaud, R. C., "Aerodynamic Whistles," Scientific America, 222, No. 1, pp 40-46, 1970.

44. Wilson, T. A., et al, "Experiments on the Fluid Mechanisms of Whistling," Vol. 51, No. 1 (Pt 2), 1971.

45. Crow, S. C., and F. H. Champagne, "Orderly Structure in Jet Turbulence," J. Fluid Mech., Vol. 48, Pt 3, pp 547-591, 1971.

46. Olsen, W. A., et al, "Noise Generated by Impingement of a Jet Upon a Large Flat Plate," NASA TN-D-7075 (1974).

47. Von Gierke, "Uber Schneidentone an Kreisrunden Gasstrahlen und ebenen Lamellen," Zeitschrift fur angewandte Physik, Vol. 2, No. 3, March 1950.

48. Equations, Tables, and Charts for Compressible Flow, NACA Report 1153 (1953).

FIGURES

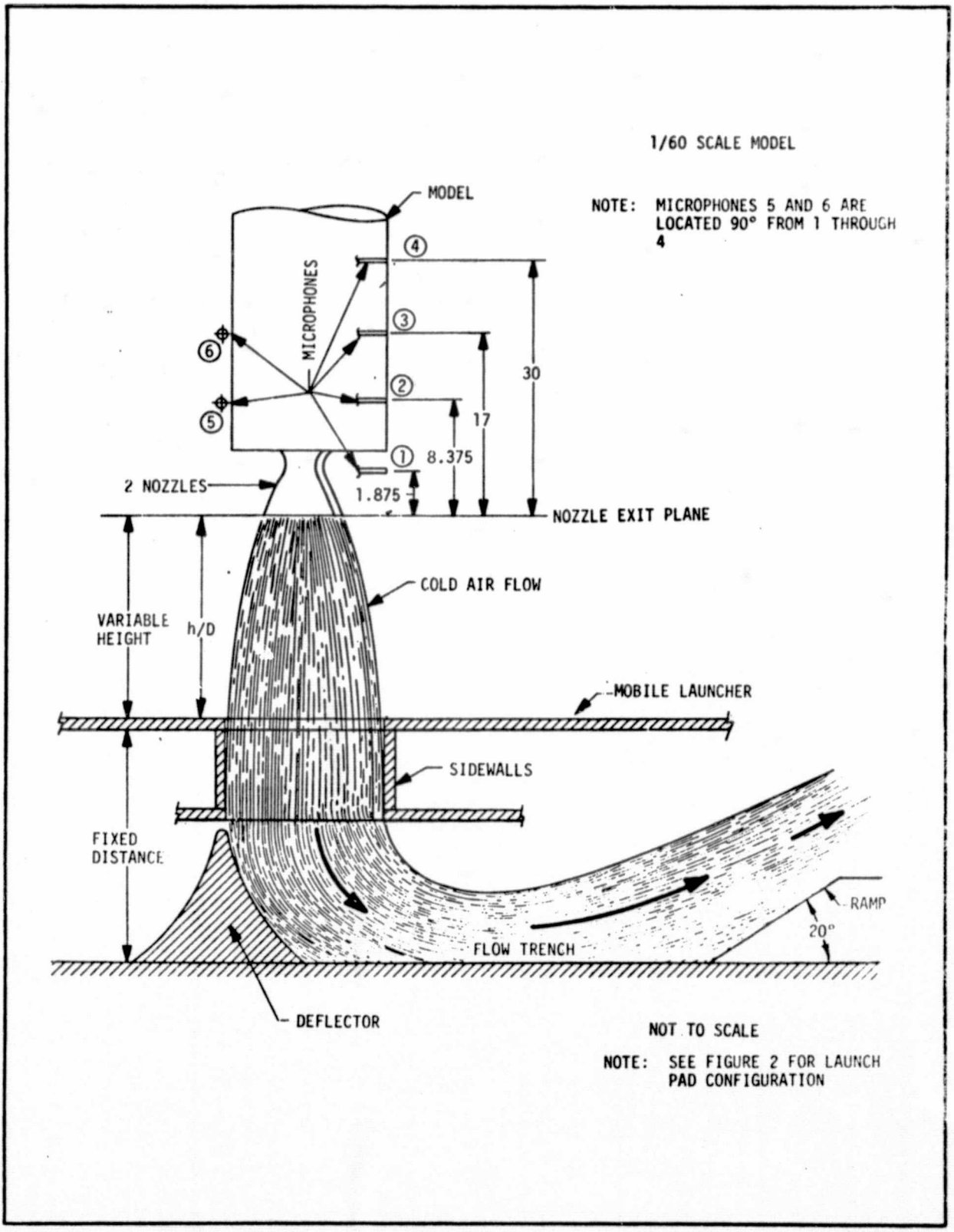

Figure 1. Model Test Arrangement

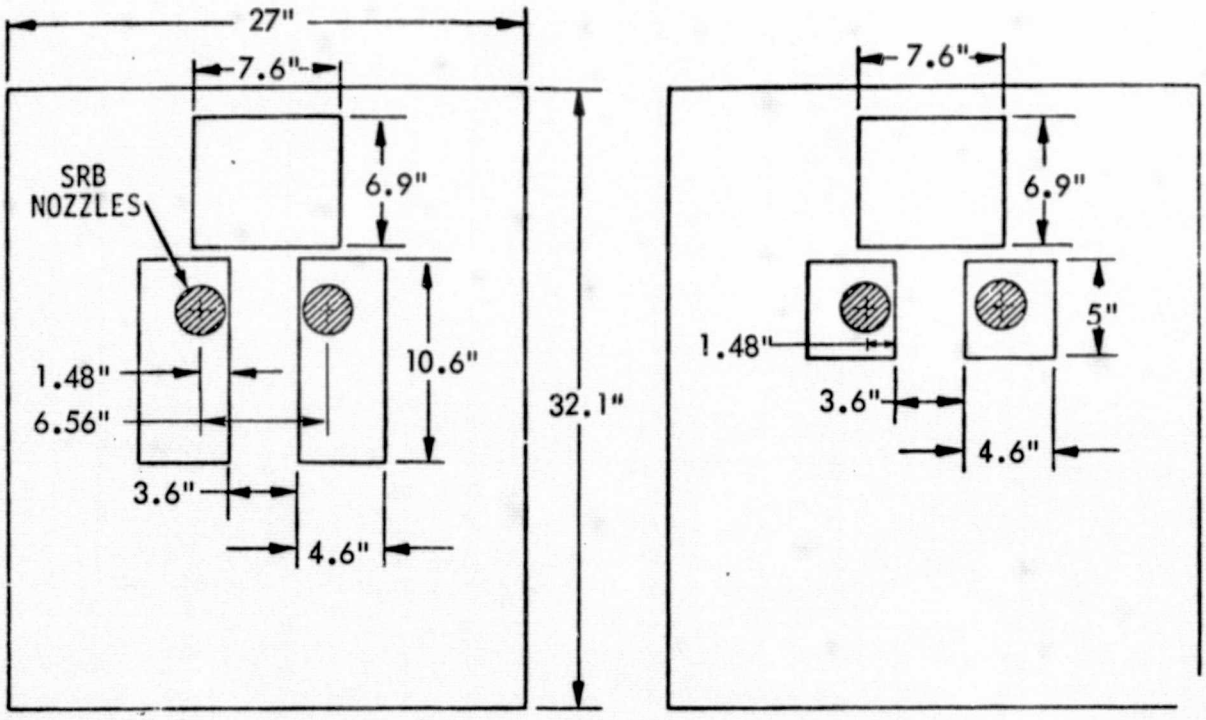

Launch Pad with Nominal Holes

Launch Pad with
Reduced Nominal Holes

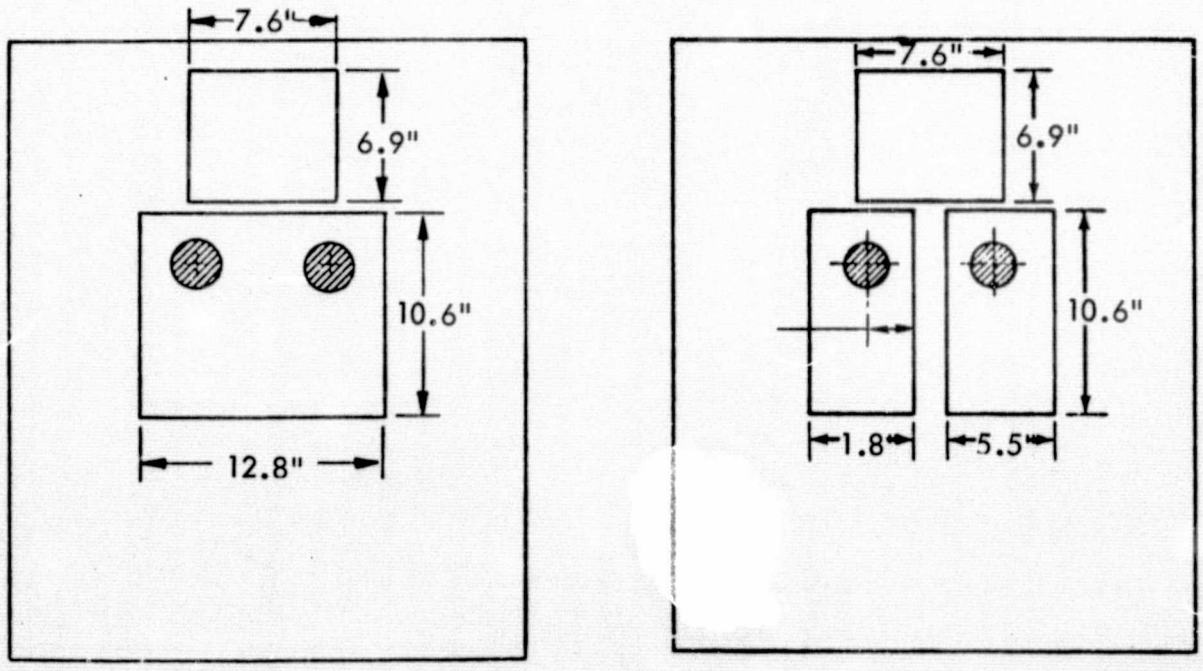

Launch Pad with
One Large SRB Hole

Launch Pad with
Widened Nominal Holes

Figure 2. Simulated Launch Pads in Model Test

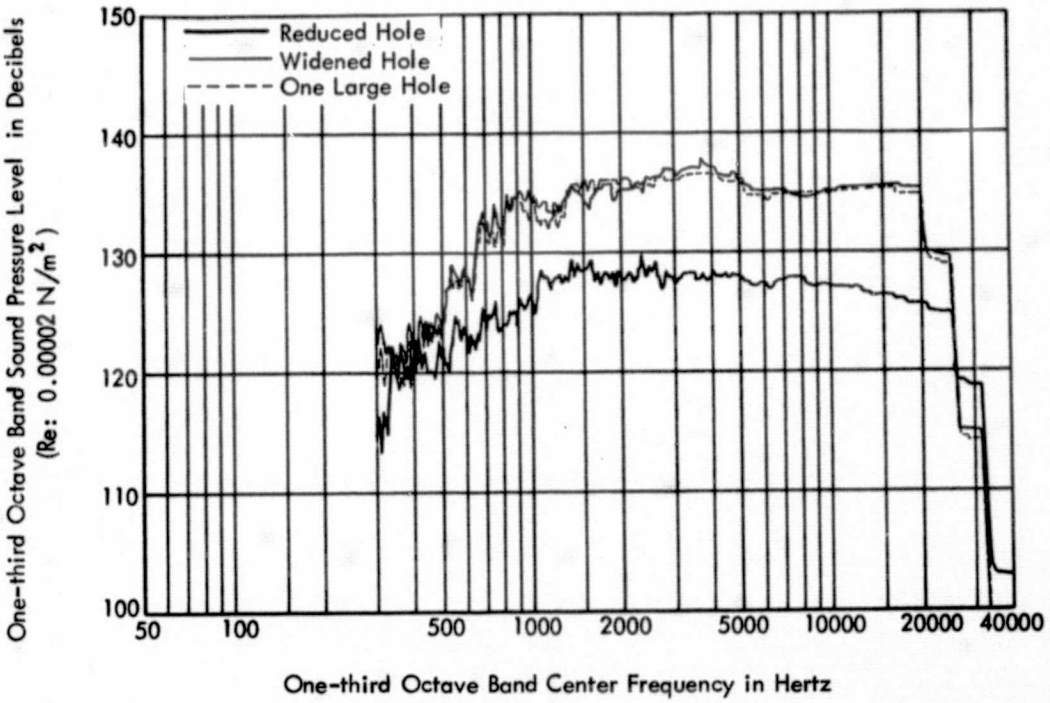

(a) Microphone No. 1

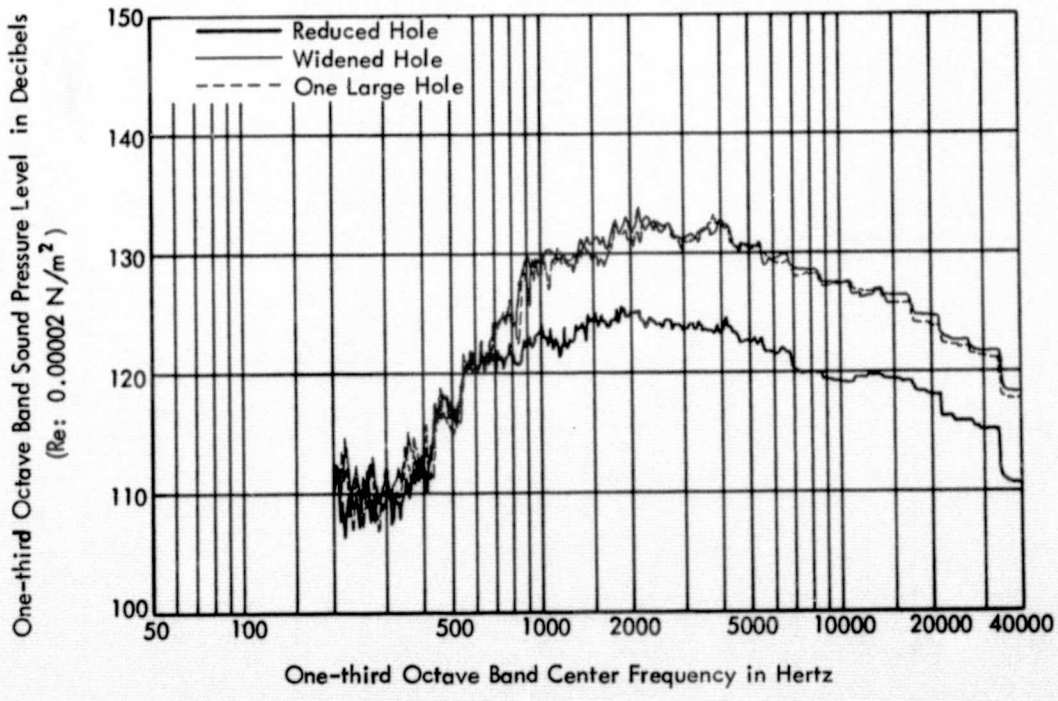

(b) Microphone No. 2

Figure 3. One-third Octave Band Sound Pressure Level Spectra for Three Launch Pad Configurations at h/D = 0

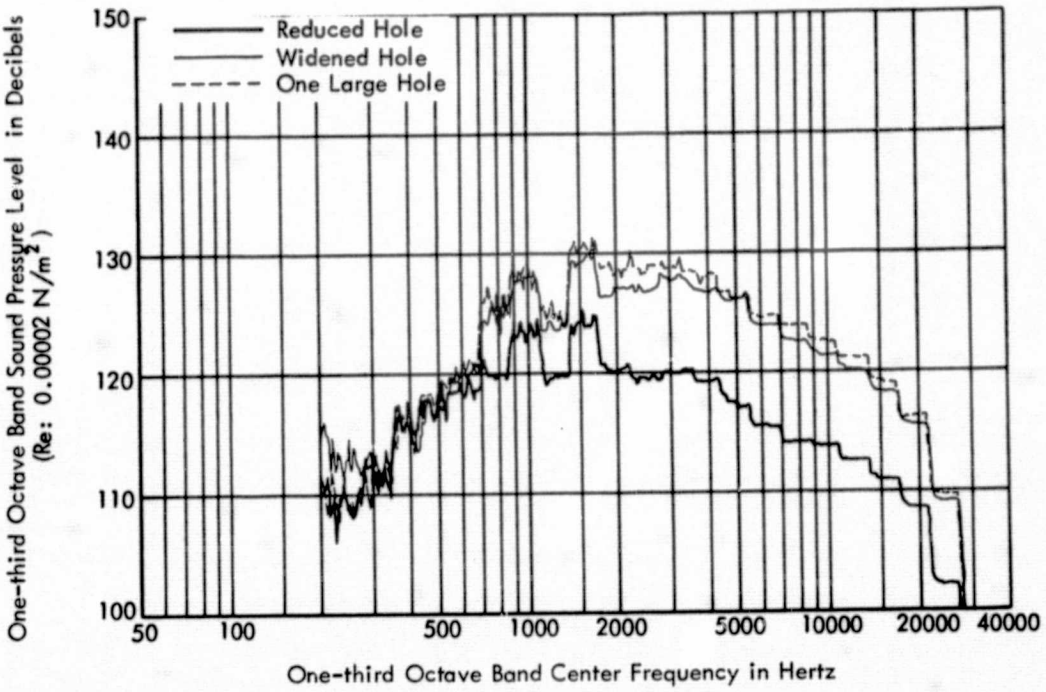

(c) Microphone No. 3

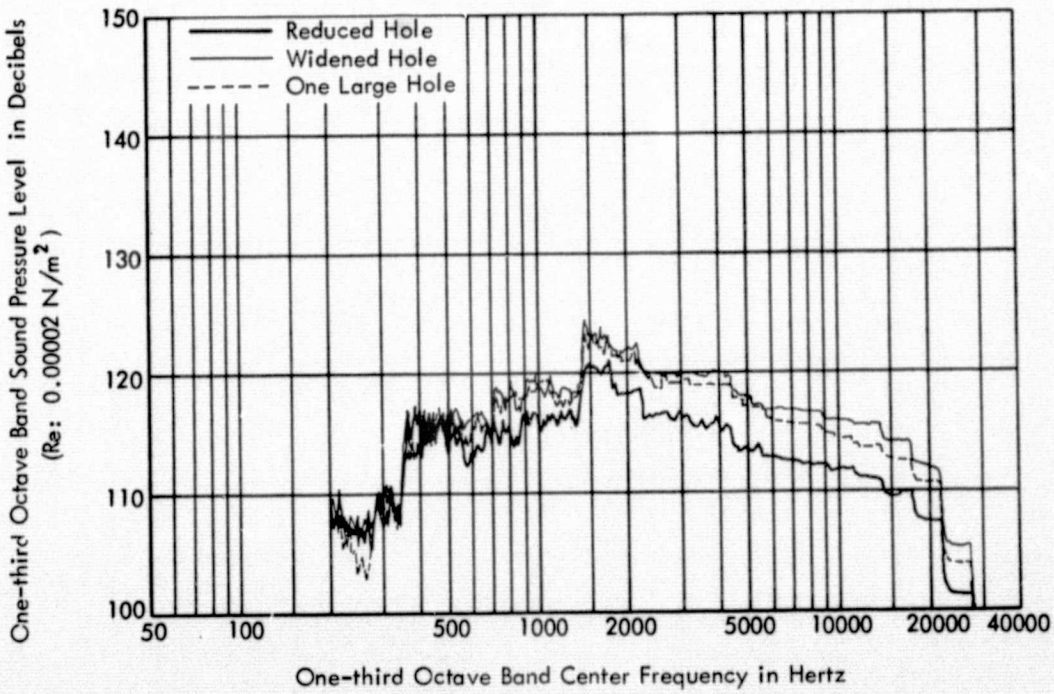

(d) Microphone No. 4

Figure 3. (Continued)

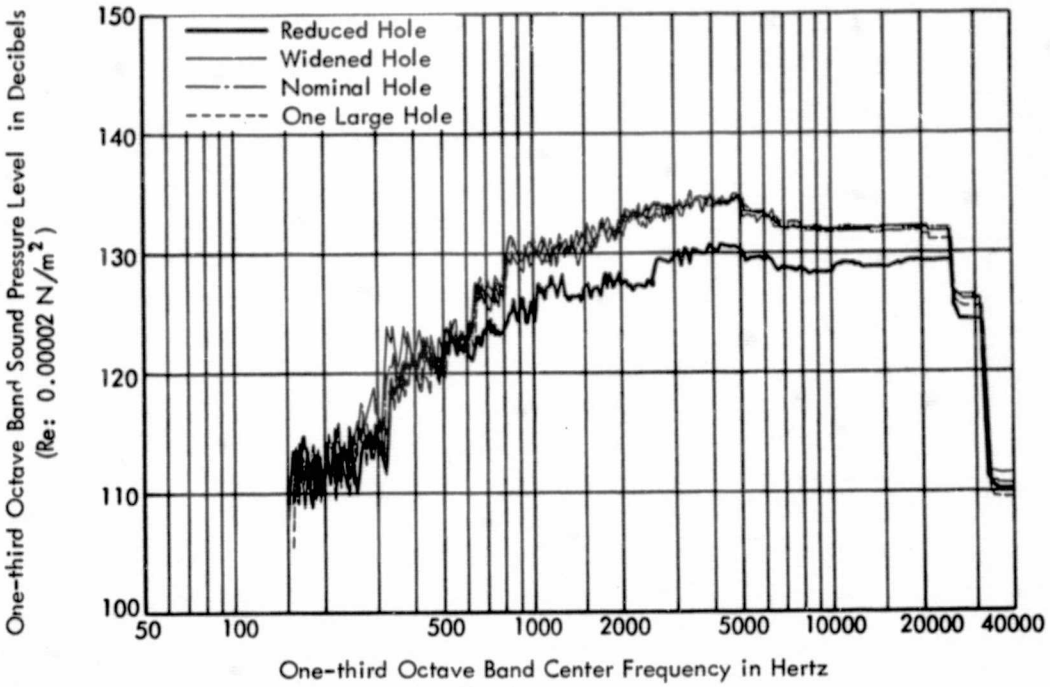

(a) Microphone No. 1

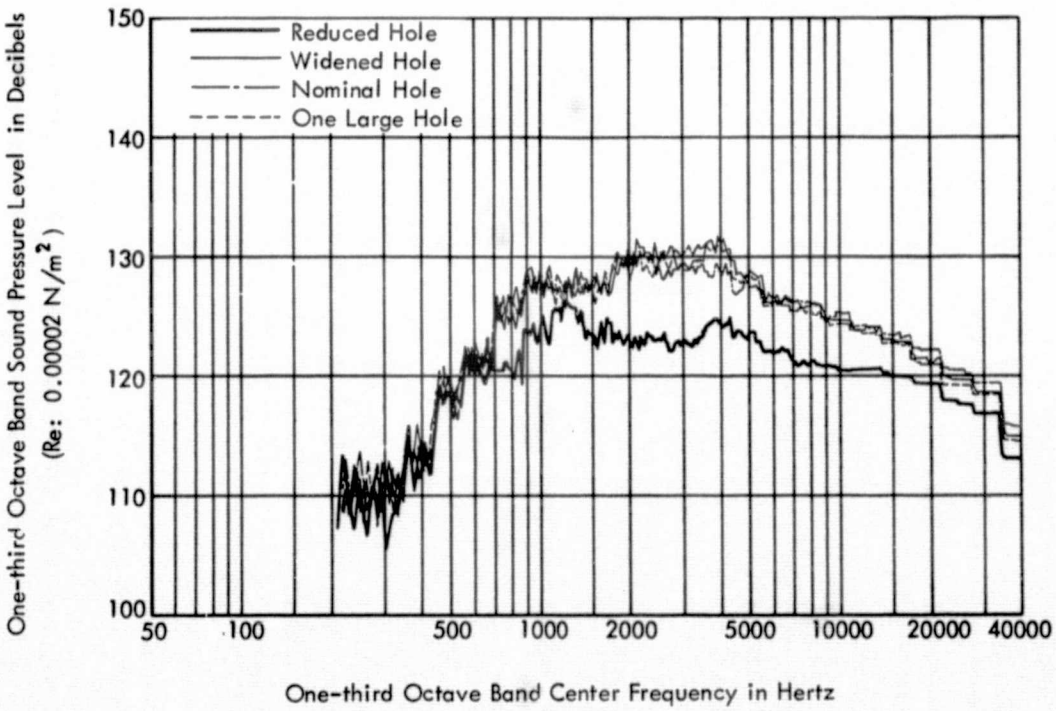

(b) Microphone No. 2

Figure 4. One-third Octave Band Sound Pressure Level Spectra for Four Launch Pad Configurations at h/D = 1

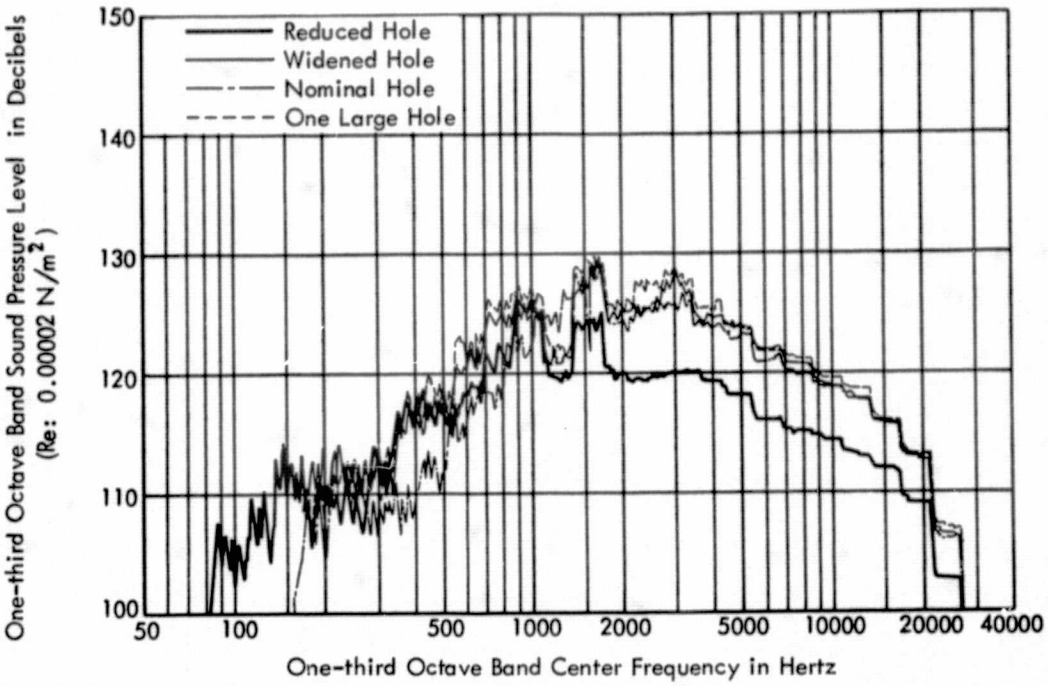

(c) Microphone No. 3

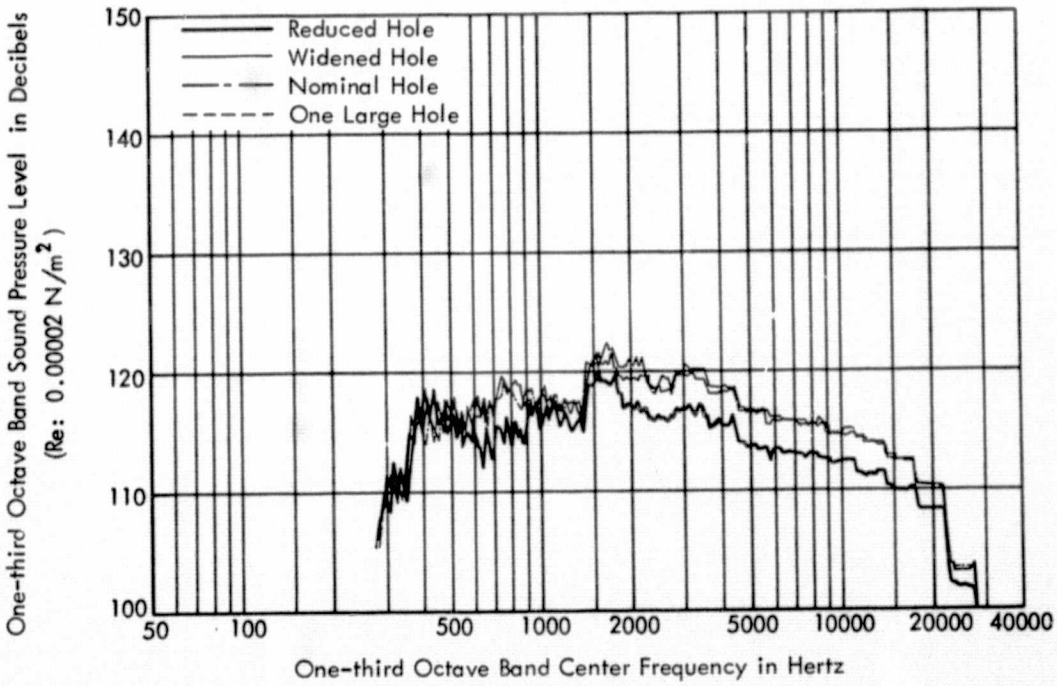

(d) Microphone No. 4

Figure 4. (Continued)

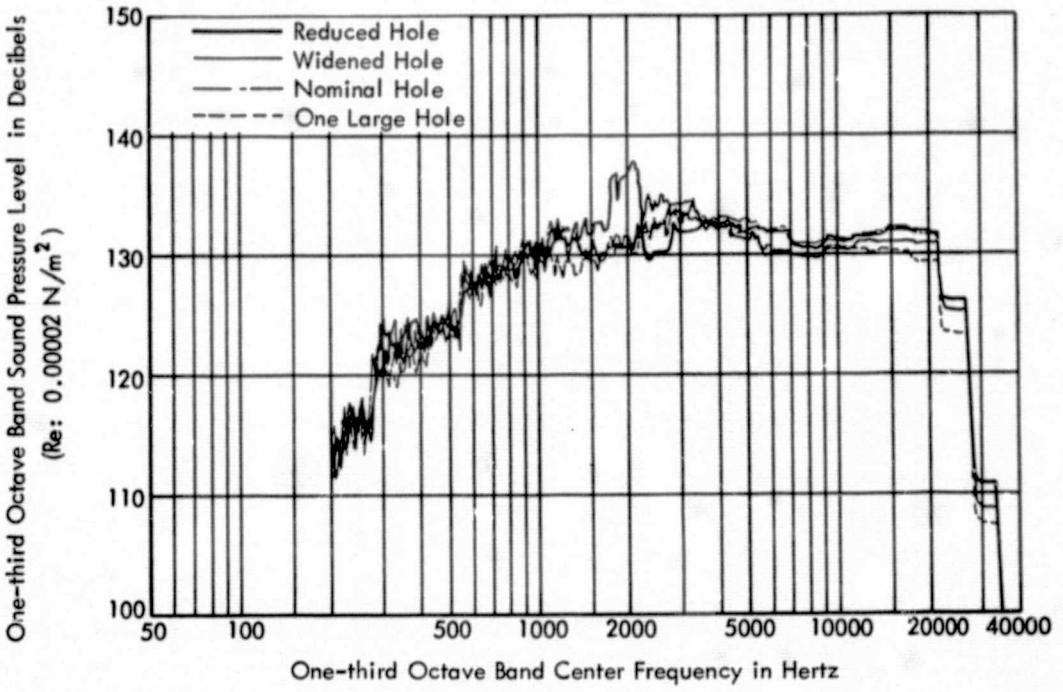

(a) Microphone No. 1

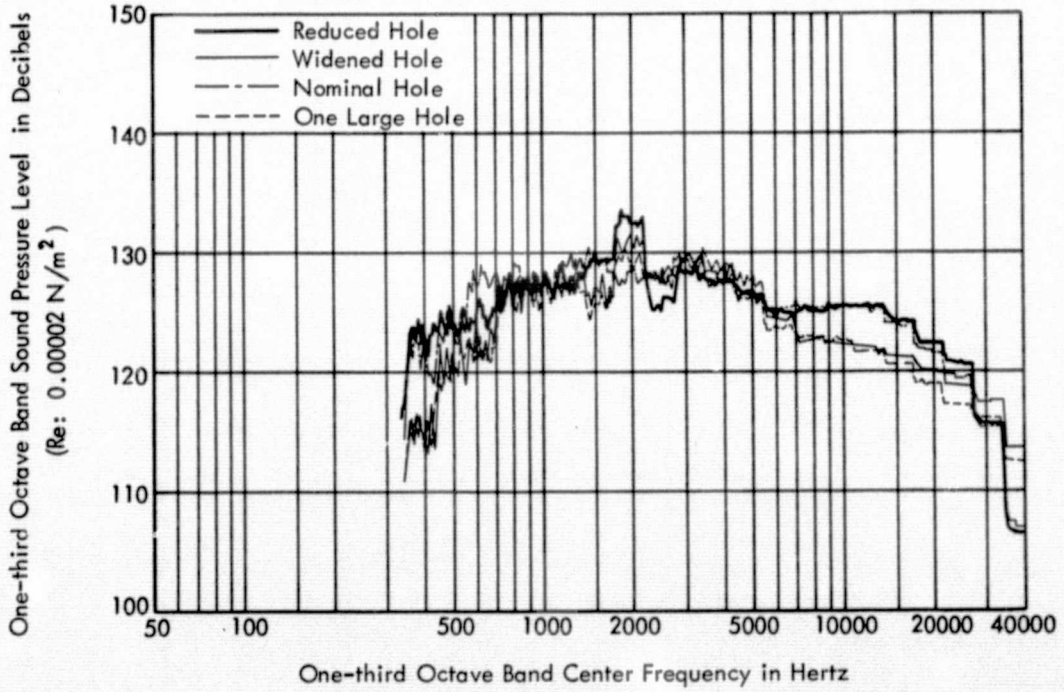

(b) Microphone No. 2

Figure 5. One-third Octave Band Sound Pressure Level Spectra for Four Launch Pad Configurations at h/D = 2

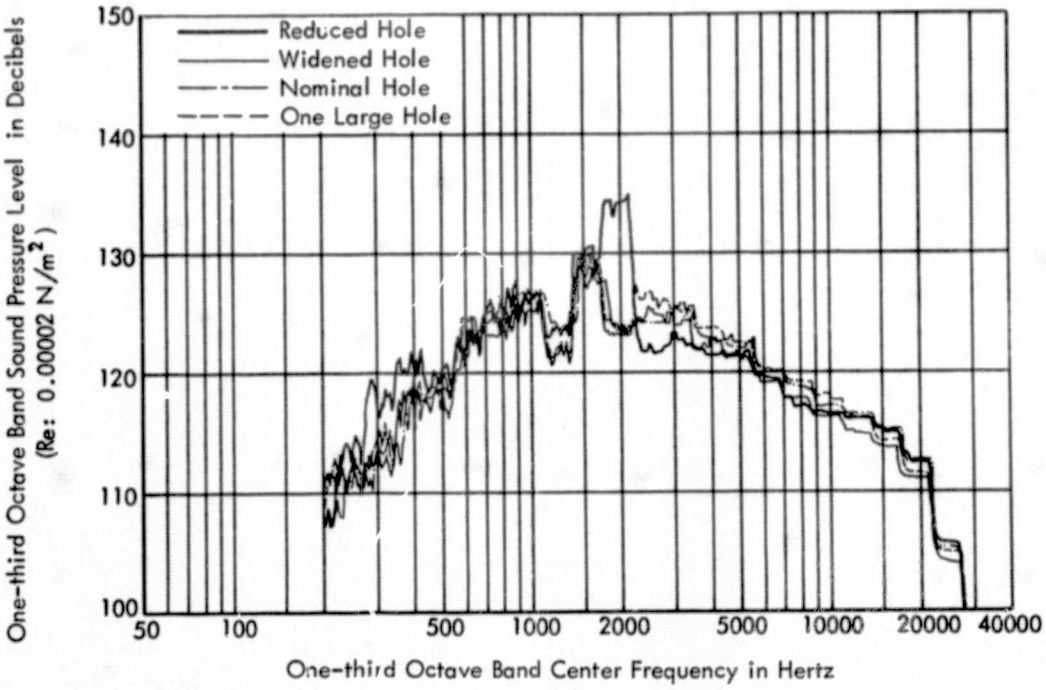

(c) Microphone No. 3

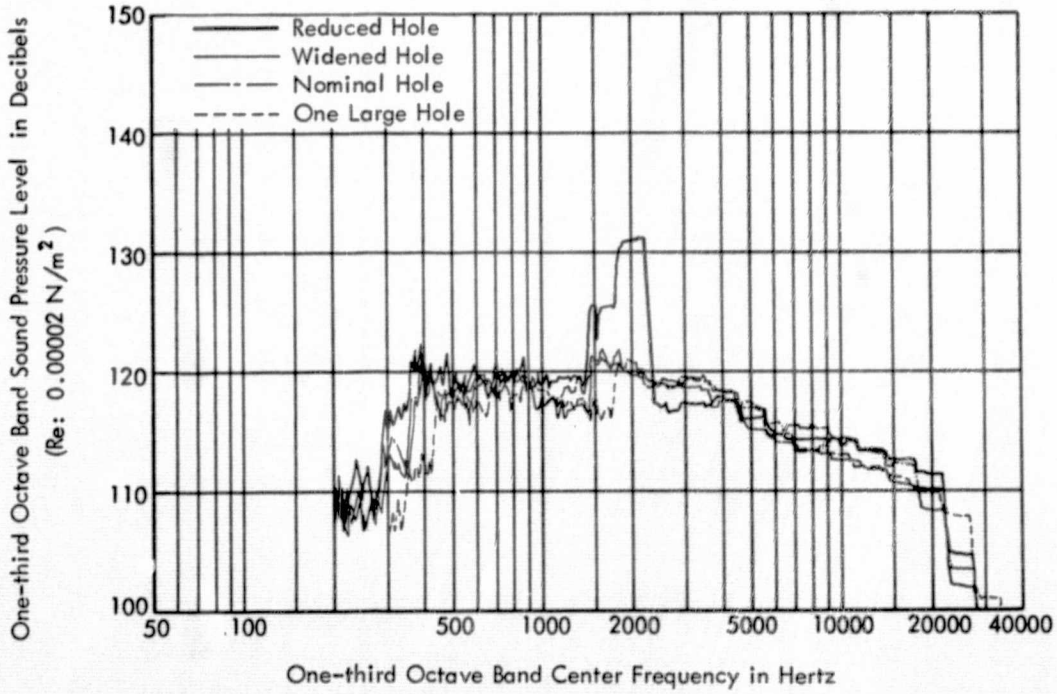

(d) Microphone No. 4

Figure 5. (Continued)

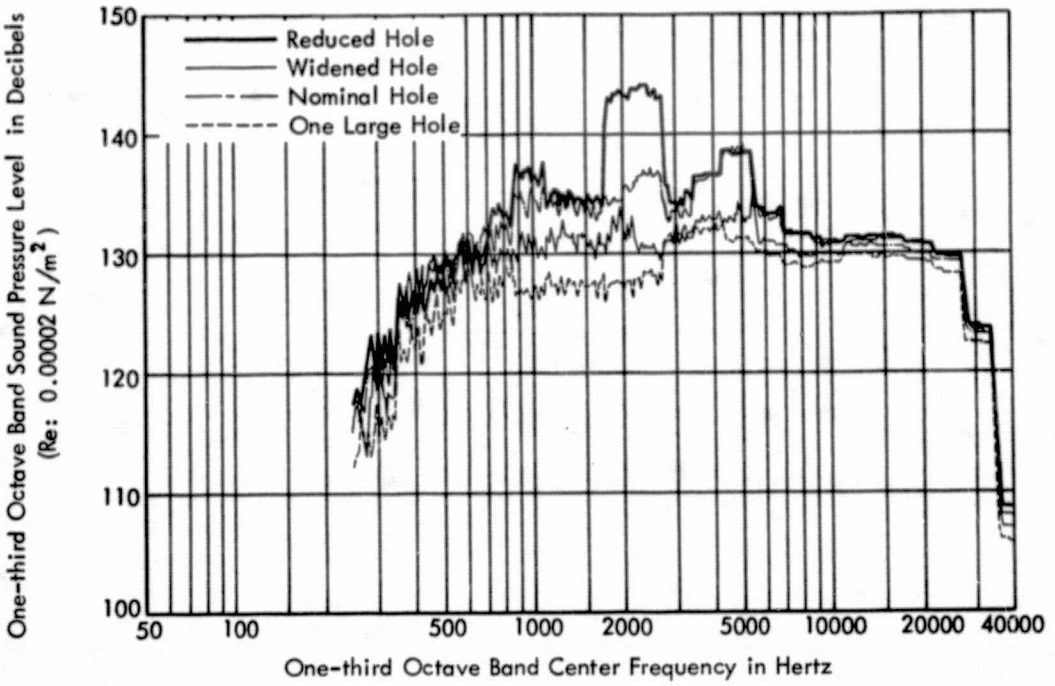

(a) Microphone No. 1

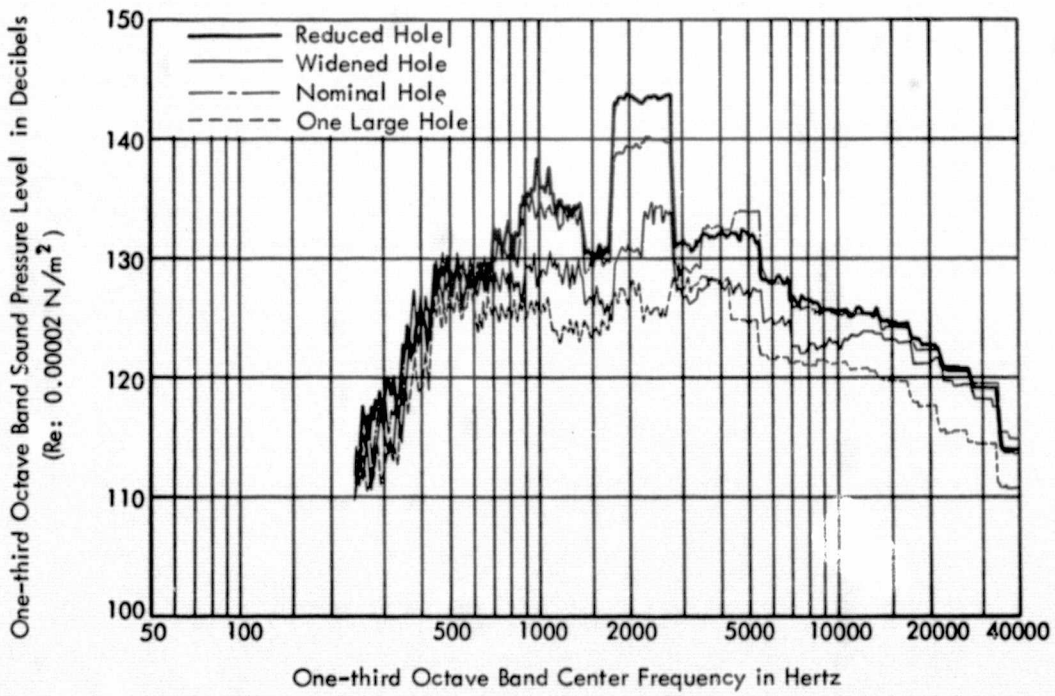

(b) Microphone No. 2

Figure 6. One-third Octave Band Sound Pressure Level Spectra for Four Launch Pad Configurations at h/D = 4

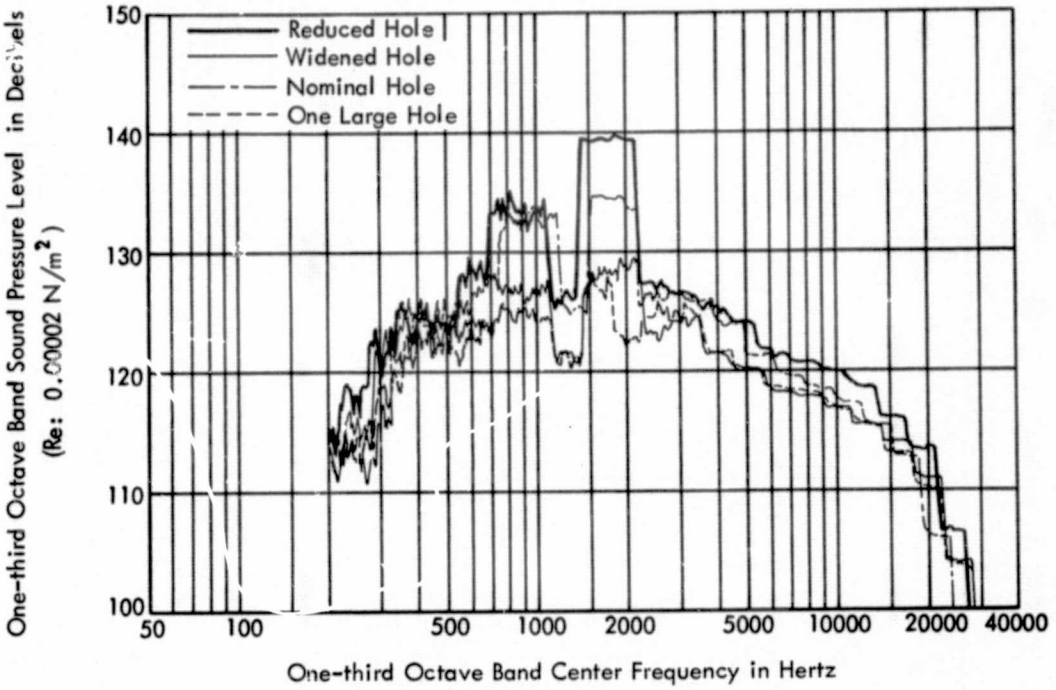

(c) Microphone No. 3

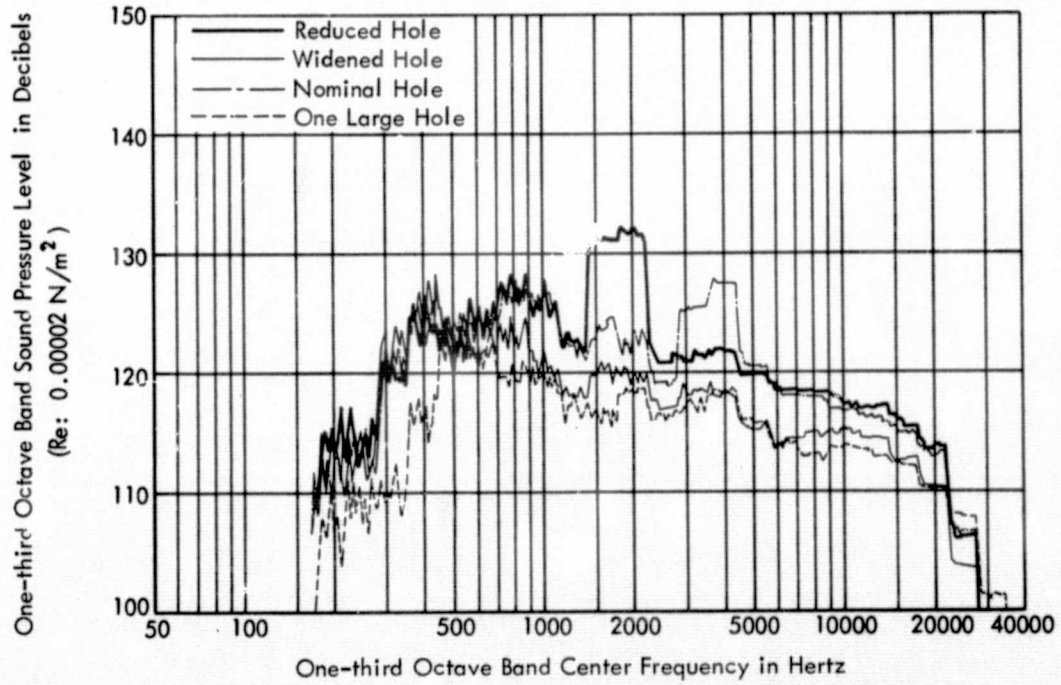

(d) Microphone No. 4

Figure 6. (Continued)

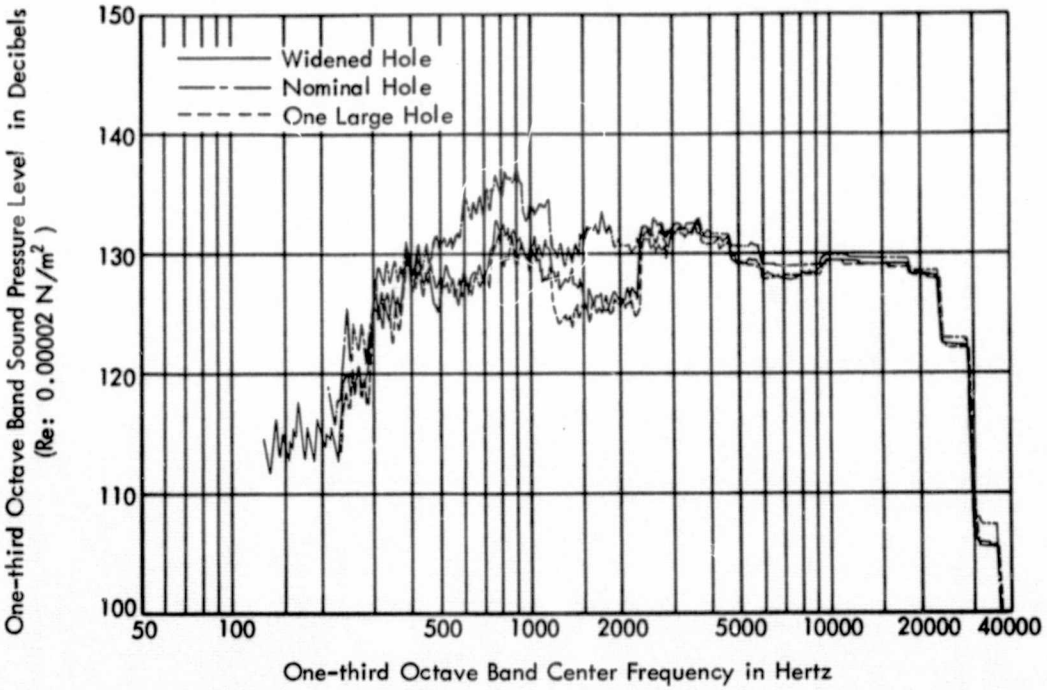

(a) Microphone No. 1

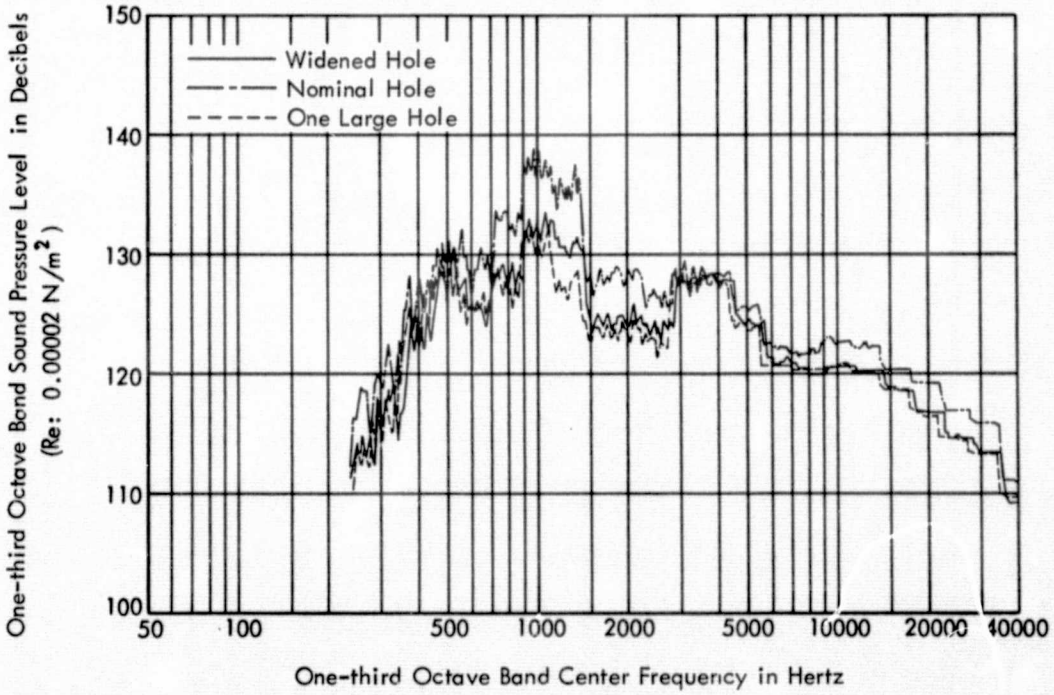

(b) Microphone No. 2

Figure 7. One-third Octave Band Sound Pressure Level Spectra for Three Launch Pad Configurations at h/D = 8

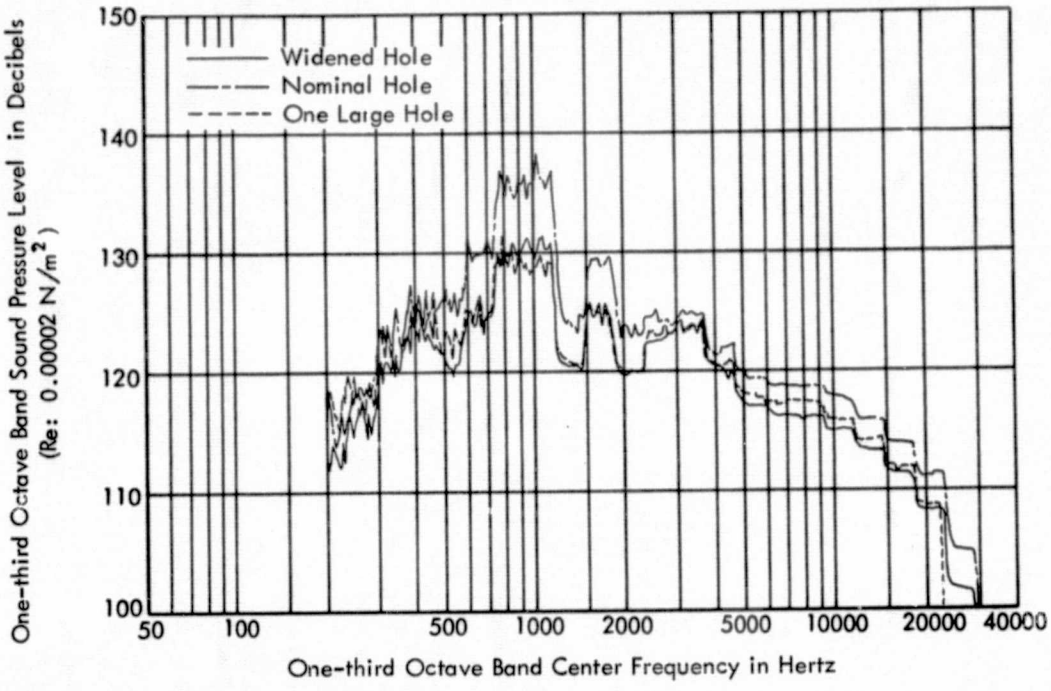

(c) Microphone No. 3

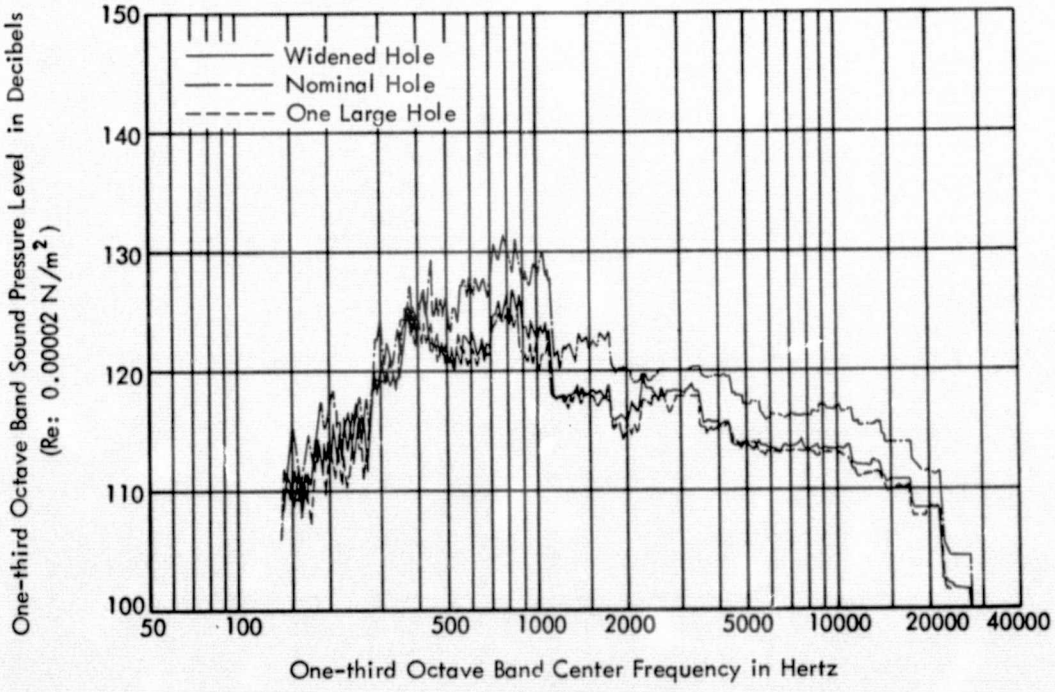

(d) Microphone No. 4

Figure 7. (Continued)

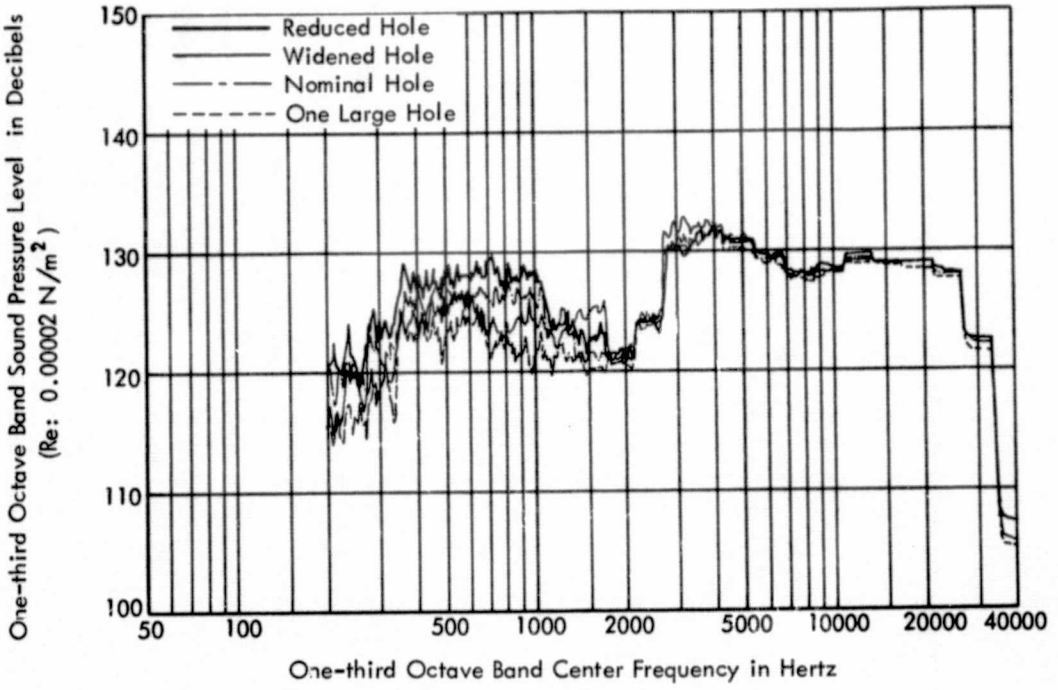

(a) Microphone No. 1

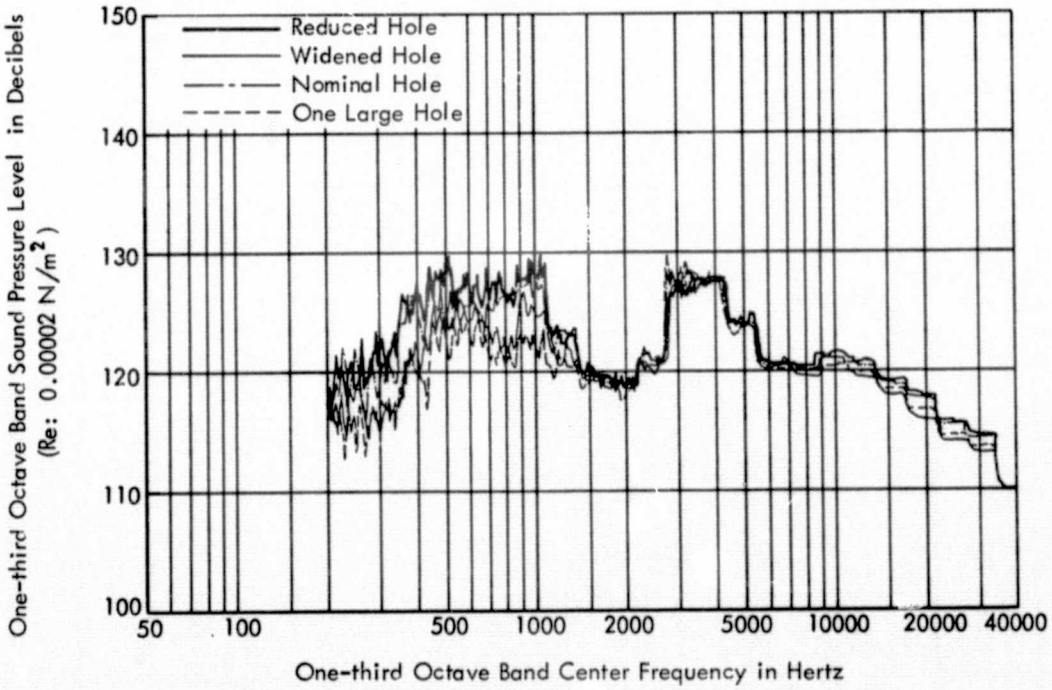

(b) Microphone No. 2

Figure 8. One-third Octave Band Sound Pressure Level Spectra for Four Launch Pad Configurations at h/D = 16

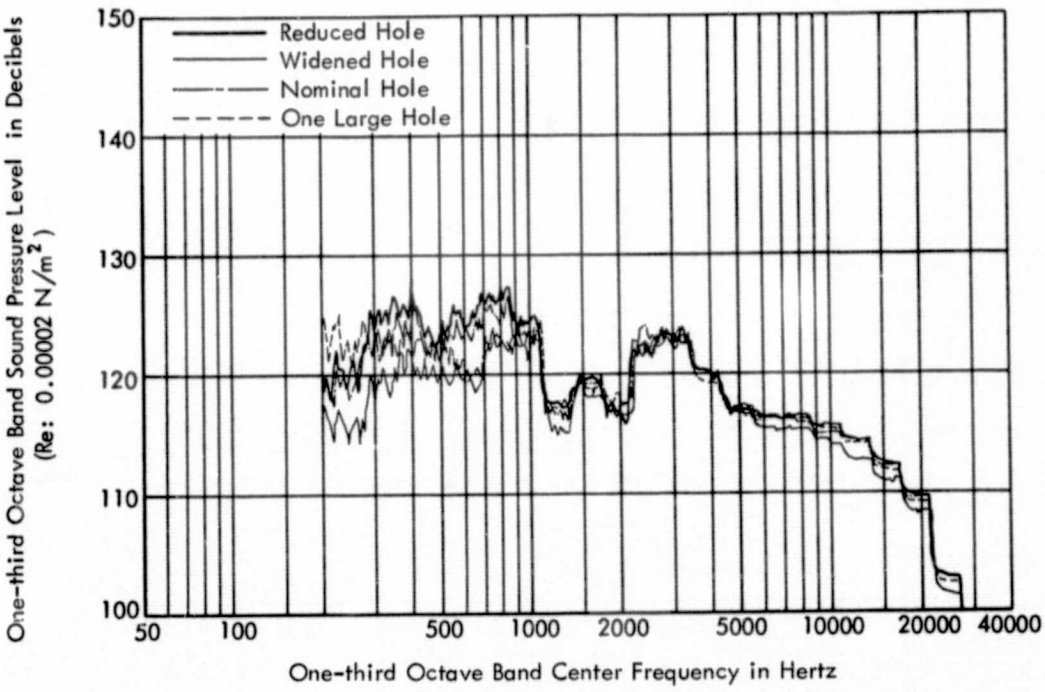

(c) Microphone No. 3

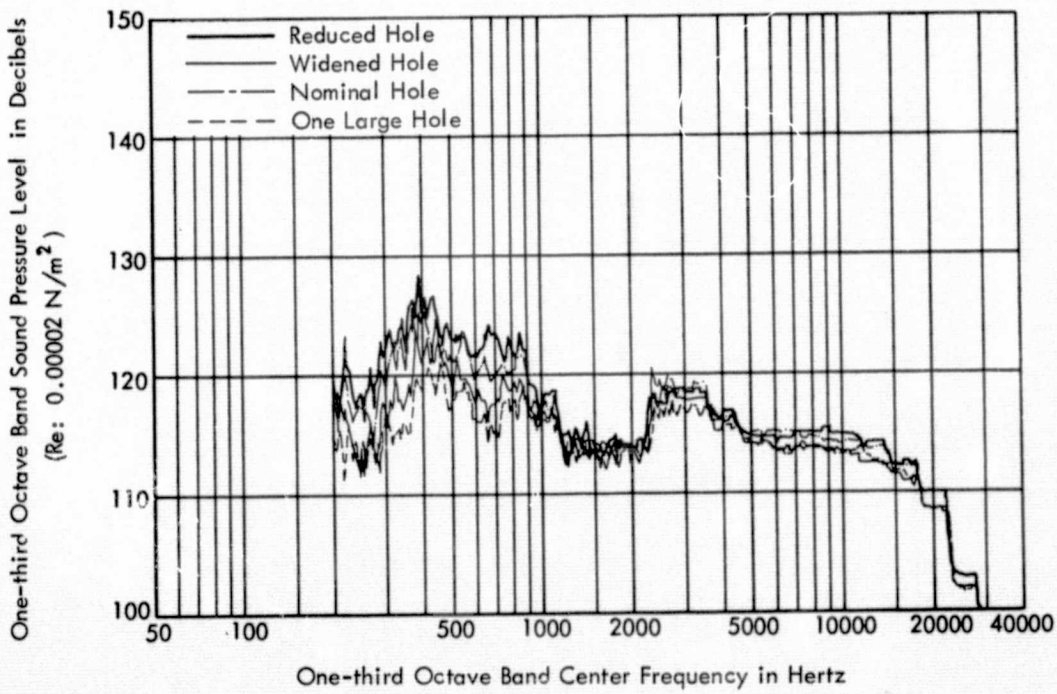

(d) Microphone No. 4

Figure 8. (Continued)

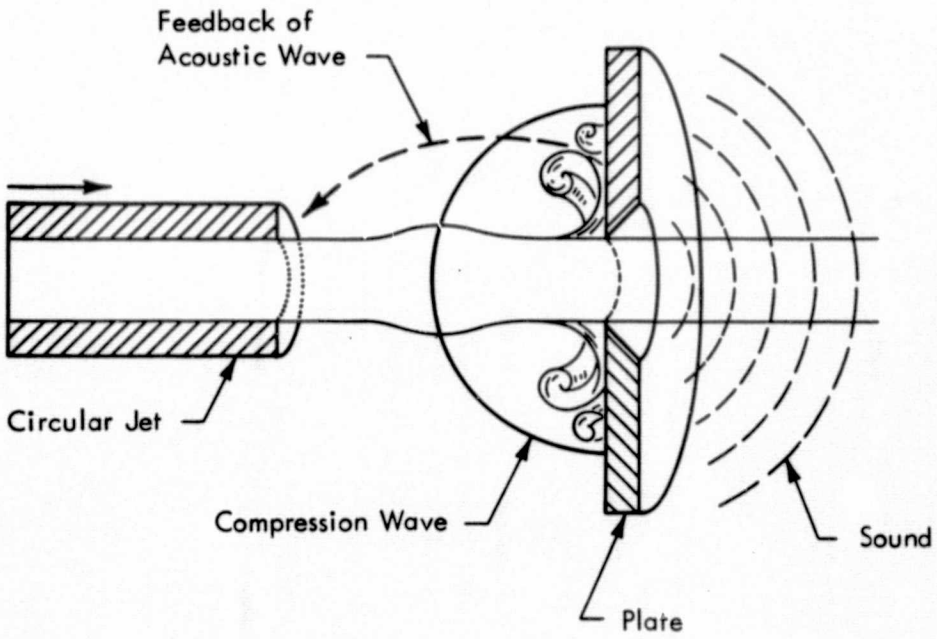

(a) Hole Tone Generating Mechanism
(Reproduced from Reference 43)

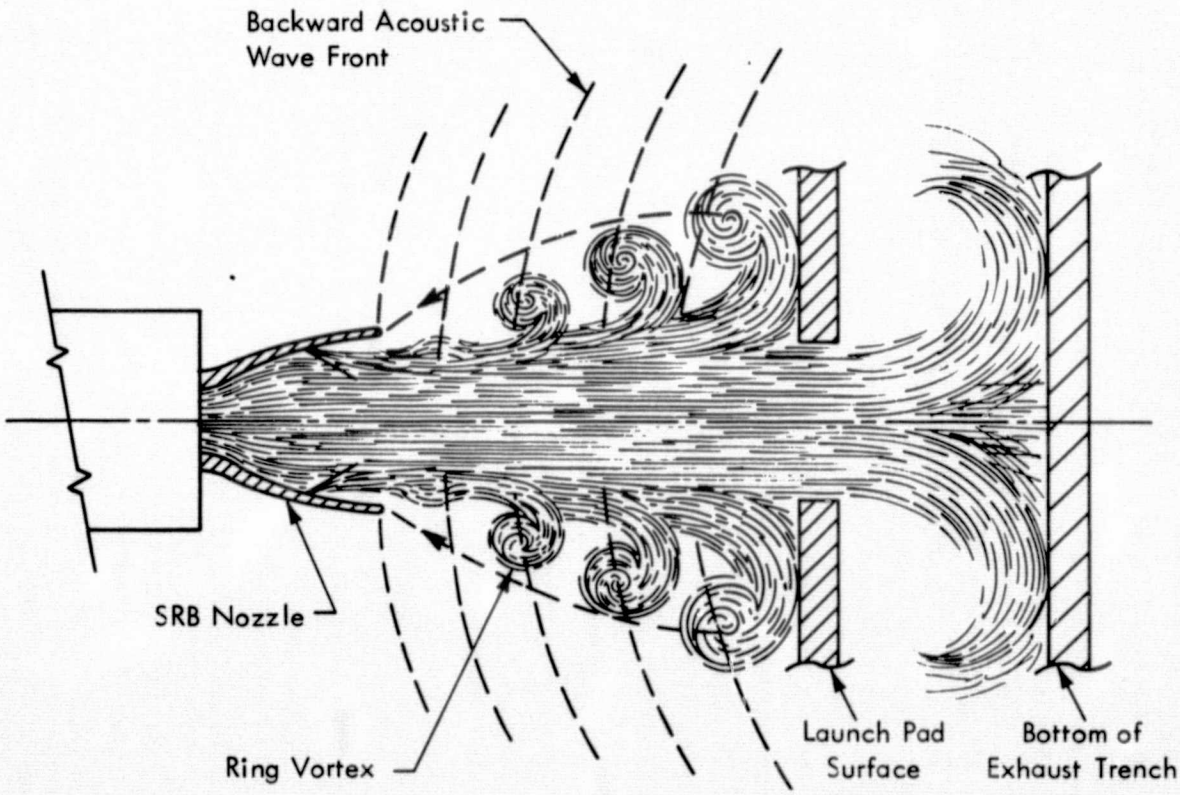

(b) MSFC Scaled Model Cold Flow Experiment

Figure 9. Schematic Representation of Hole Tone Generating Mechanism Compared to the Screech Generating Mechanism of MSFC Scaled Model Cold Flow Test

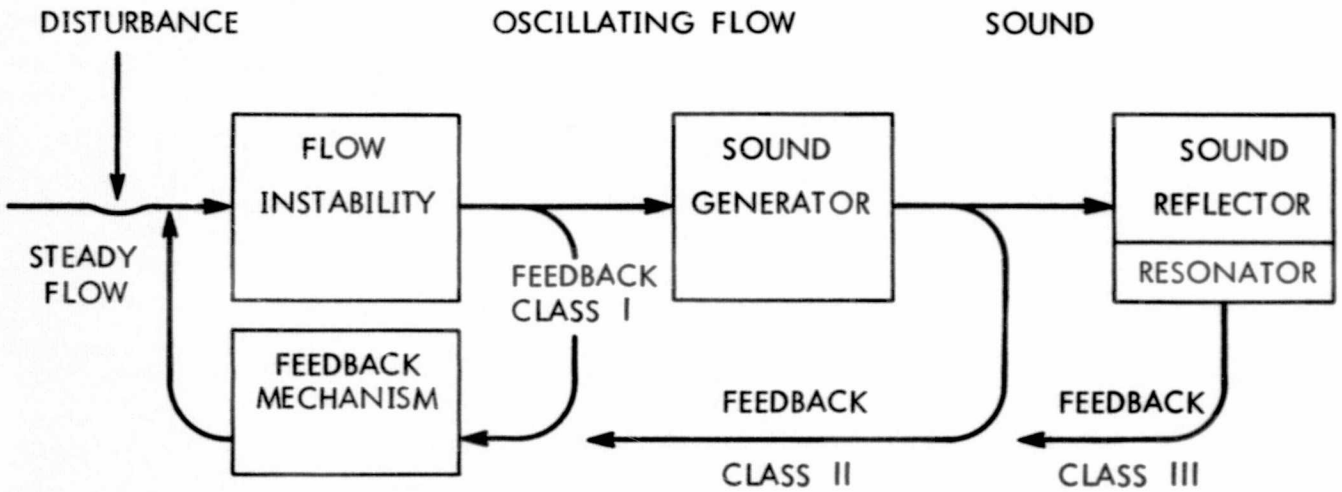

Figure 10. Block Diagram of the Aerodynamic Whistle Generating Mechanism Described by Robert Chanaud (Reference 31)

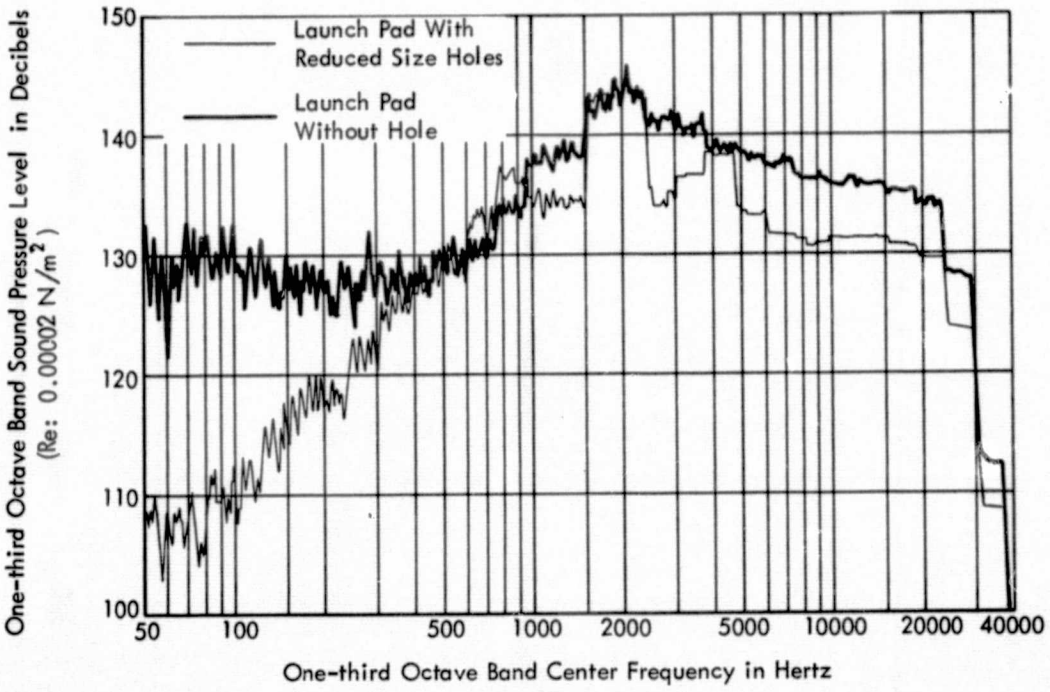

(a) Microphone No. 1

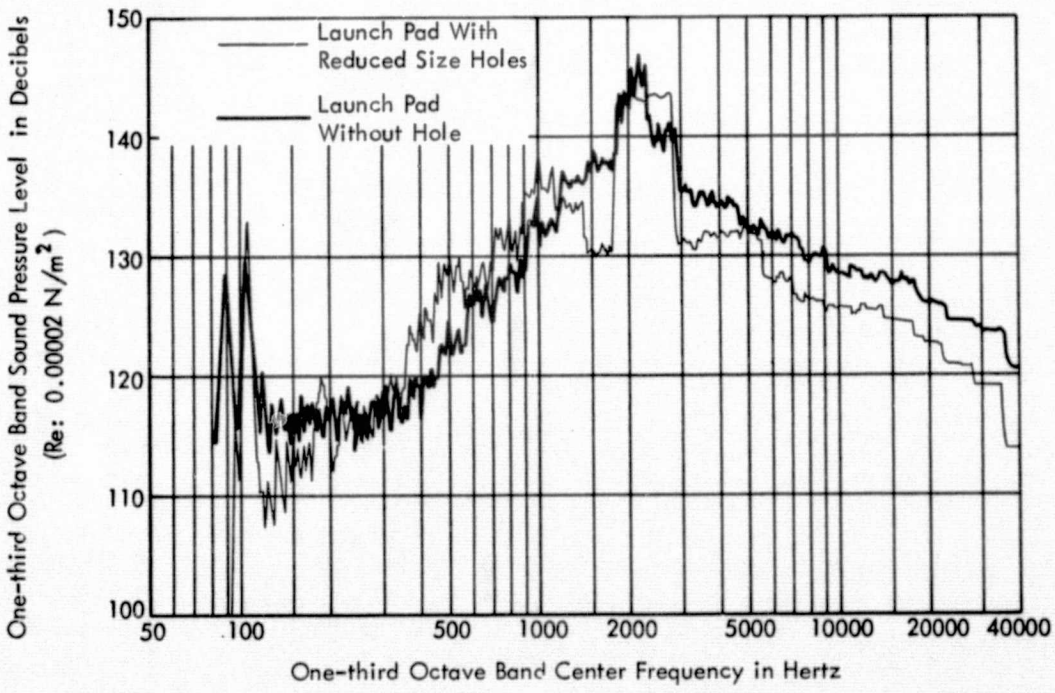

(b) Microphone No. 2

Figure 11. One-third Octave Band Sound Pressure Level Spectra for Launch Pad with Reduced Size* Exhaust Holes and for Launch Pad without Exhaust Holes (h/D = 4)

*See Figure 2.

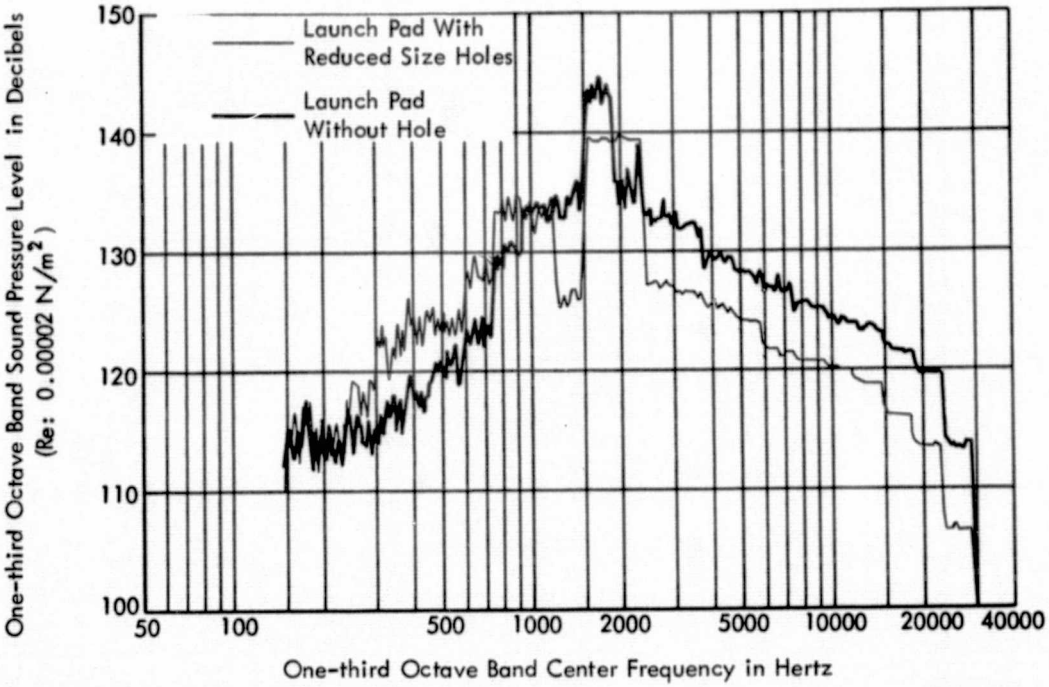

(c) Microphone No. 3

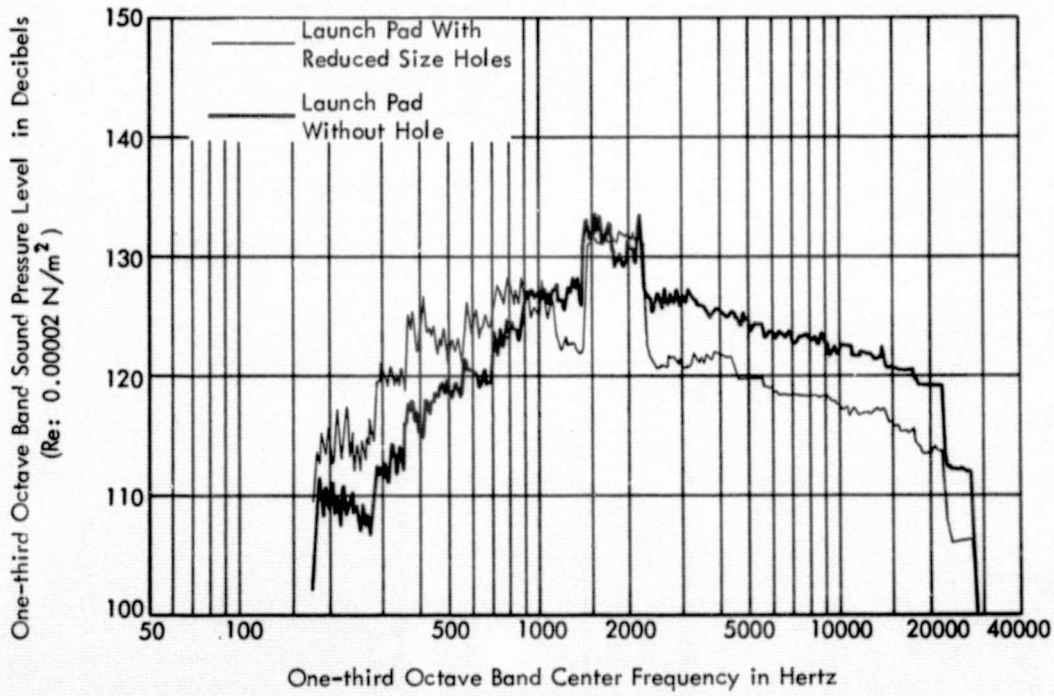

(d) Microphone No. 4

Figure 11. (Continued)

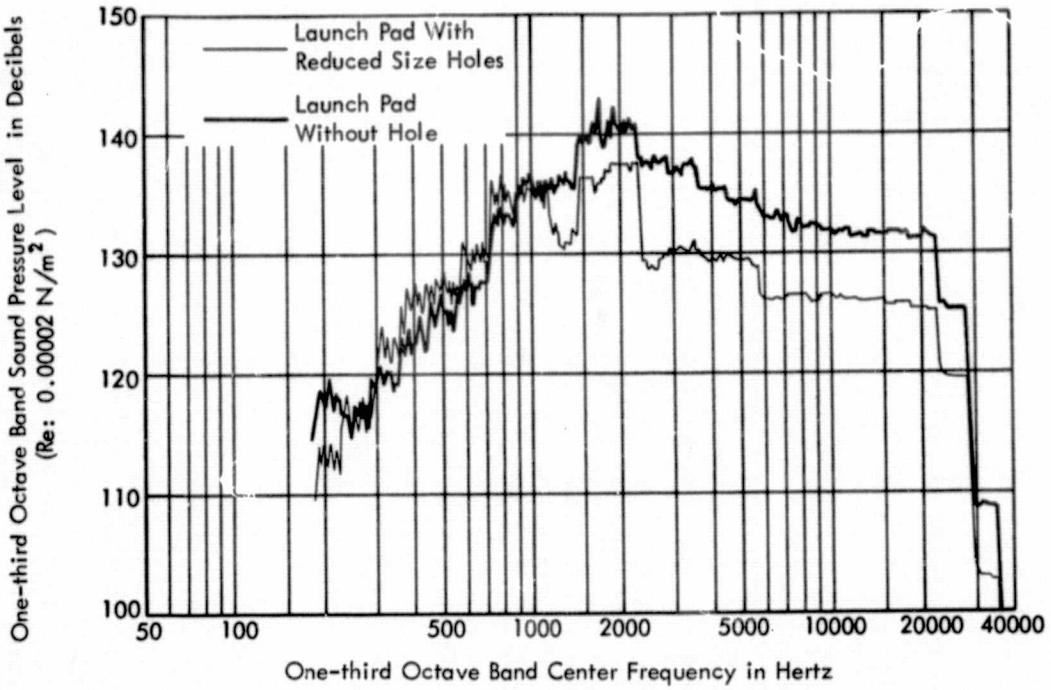

(e) Microphone No. 5

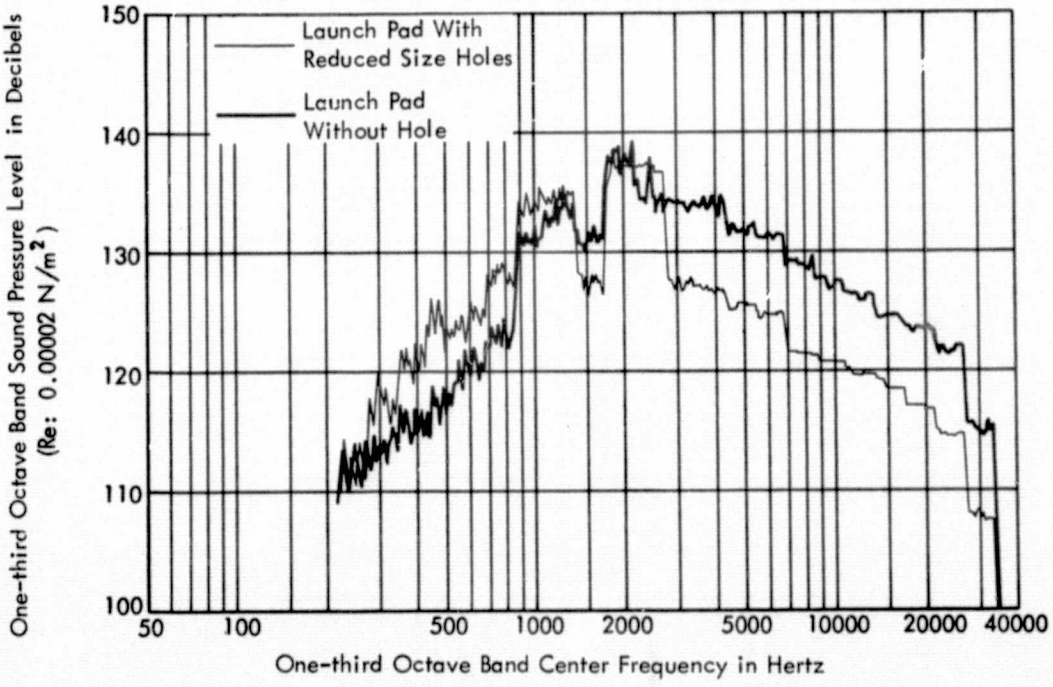

(f) Microphone No. 6

Figure 11. (Continued)

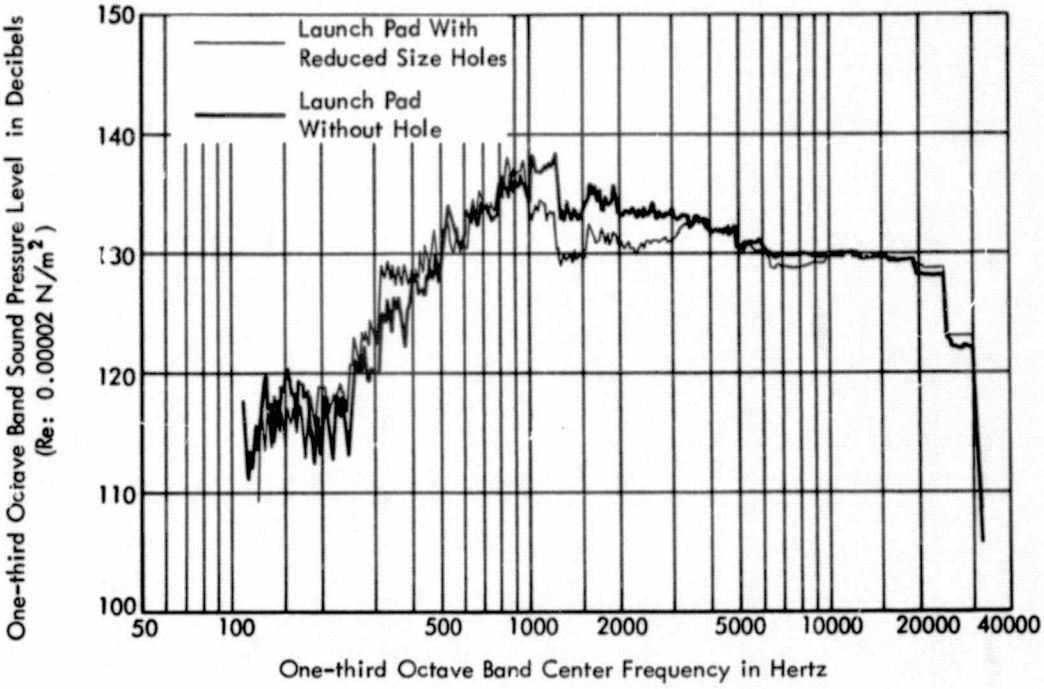

(a) Microphone No. 1

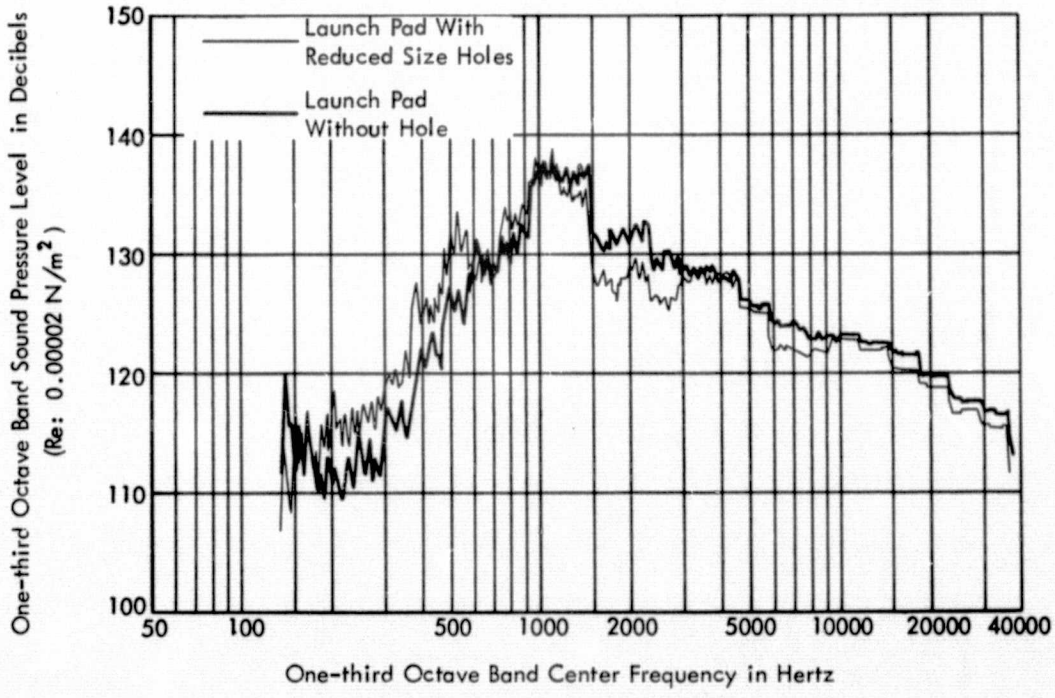

(b) Microphone No. 2

Figure 12. One-third Octave Band Sound Pressure Level Spectra for Launch Pad with Reduced Size* Exhaust Holes and for Launch Pad without Exhaust Holes (h/D = 8)

*See Figure 2.

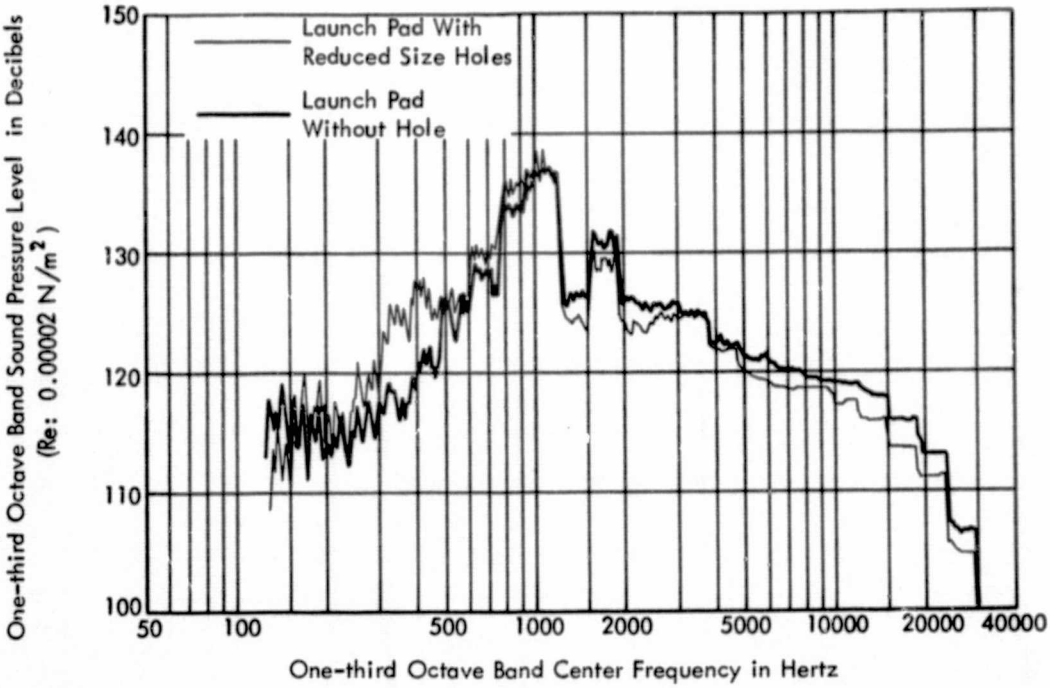

(c) Microphone No. 3

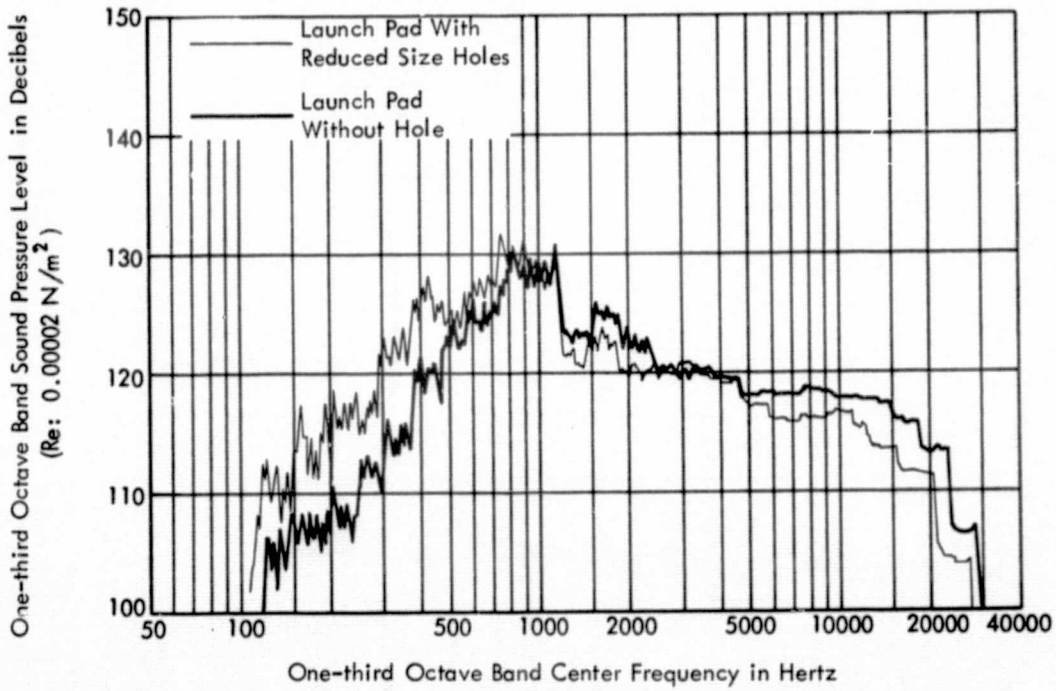

(d) Microphone No. 4

Figure 12. (Continued)

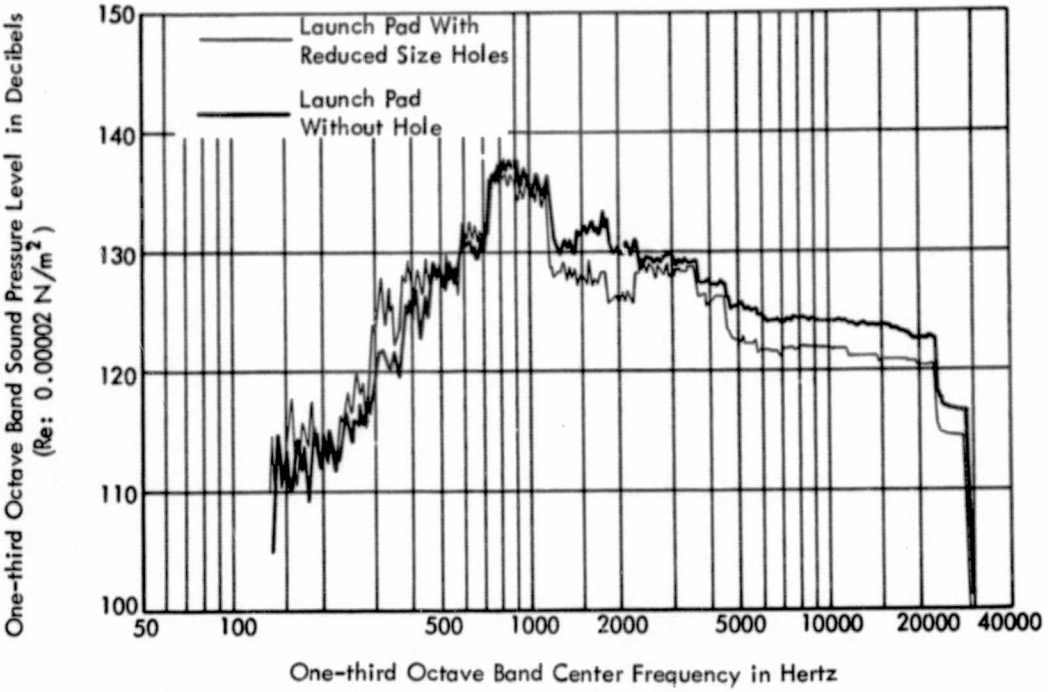

(e) Microphone No. 5

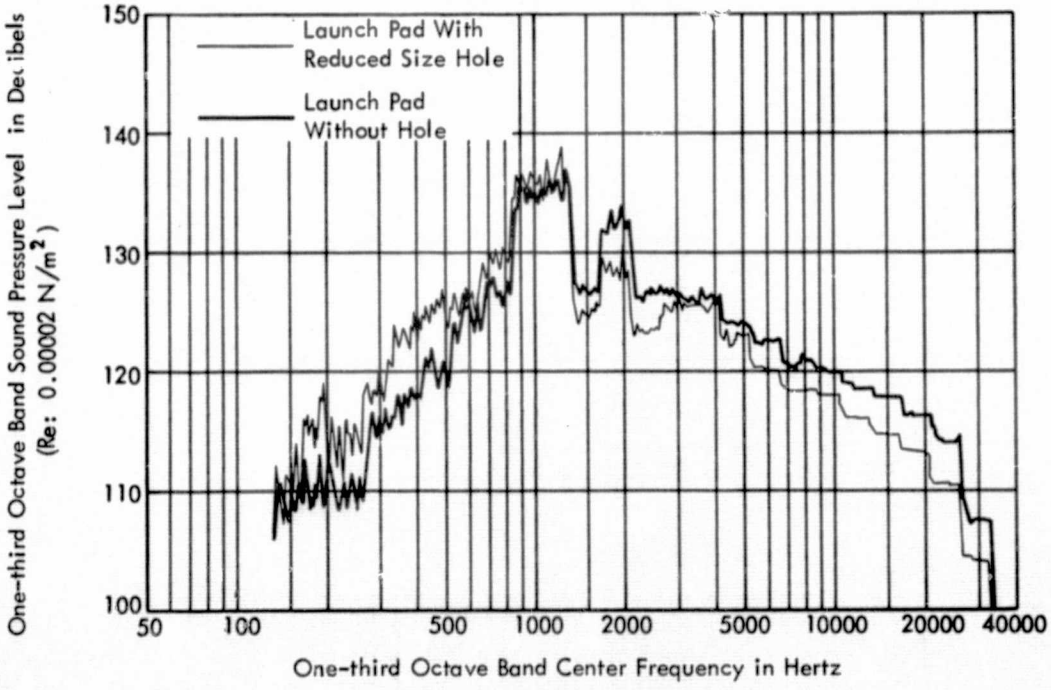

(f) Microphone No. 6

Figure 12. (Continued)

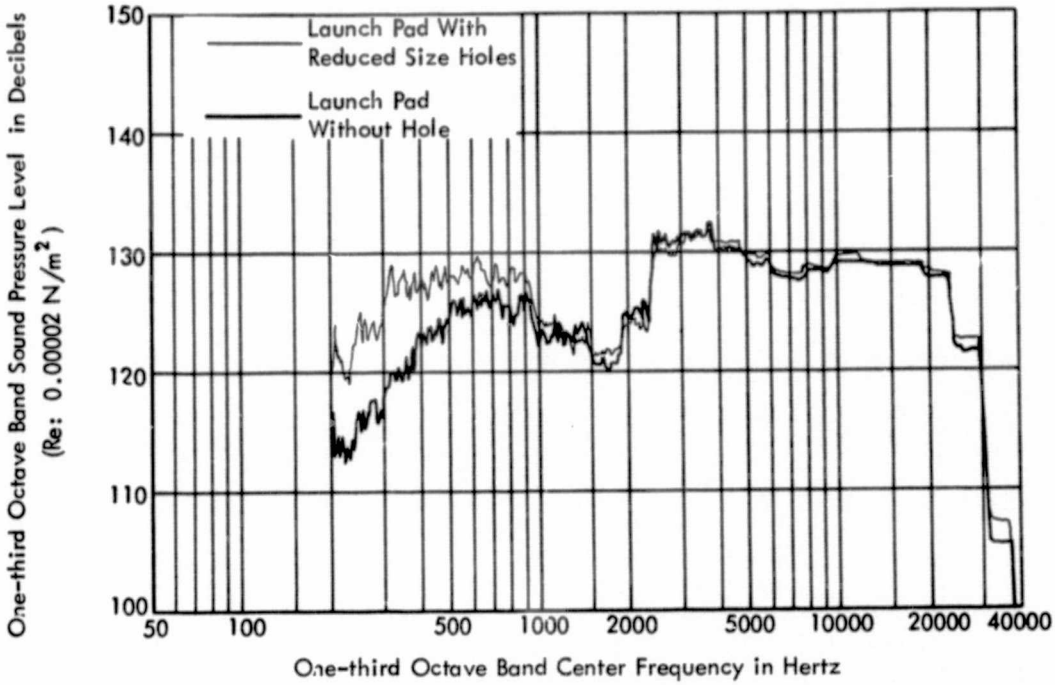

(a) Microphone No. 1

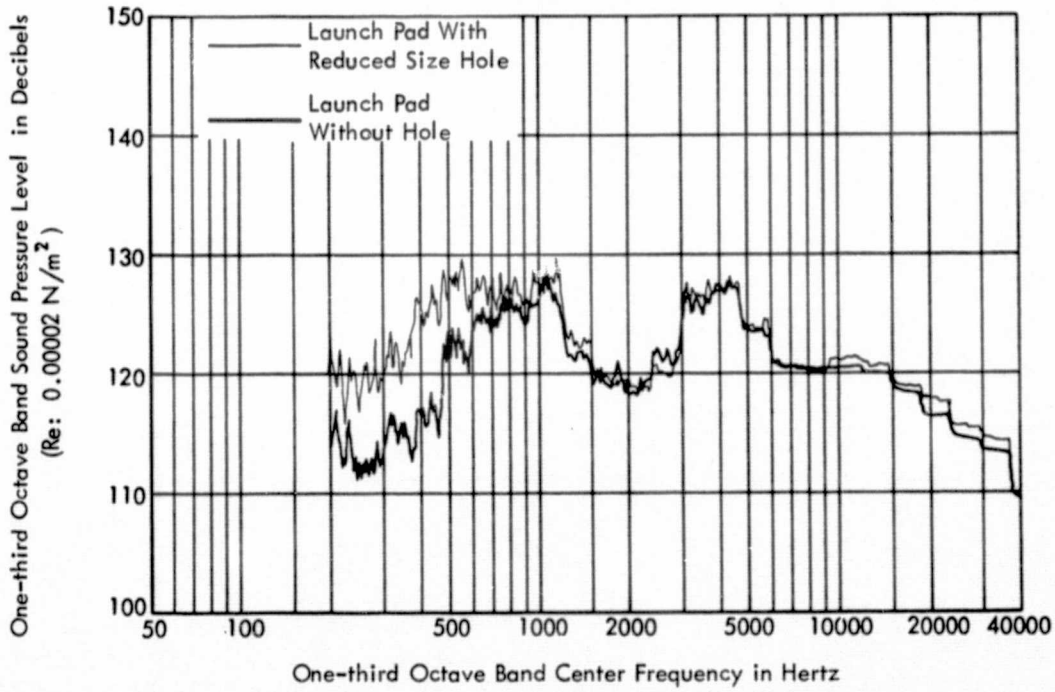

(b) Microphone No. 2

Figure 13. One-third Octave Band Sound Pressure Level Spectra for Launch Pad with Reduced Size* Exhaust Holes and for Launch Pad without Exhaust Holes (h/D = 16)

*See Figure 2.

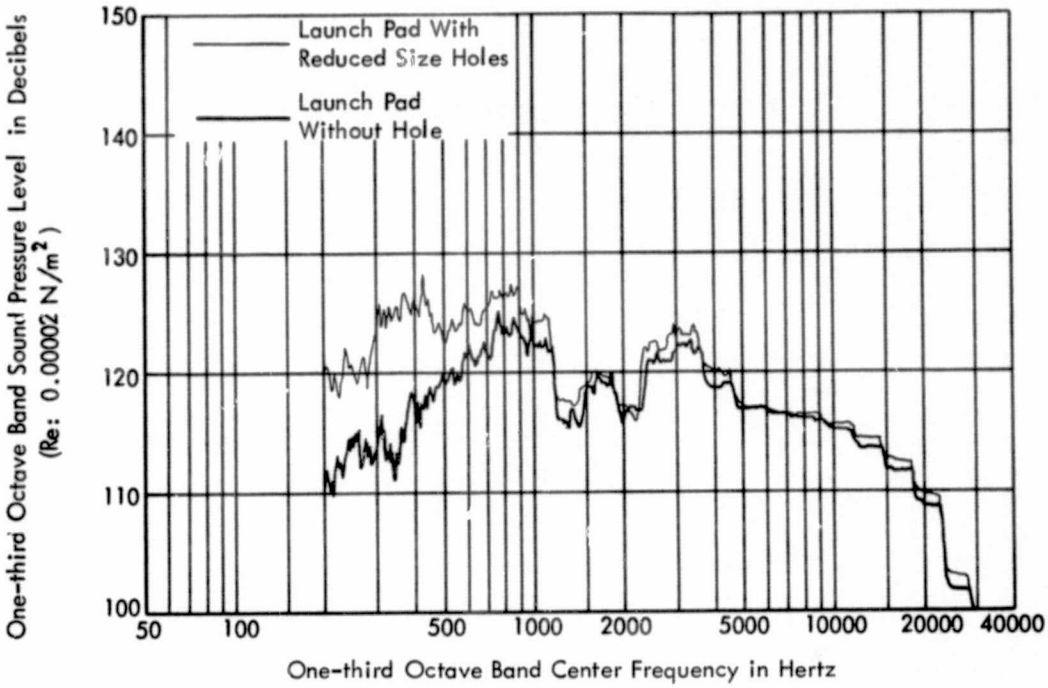

(c) Microphone No. 3

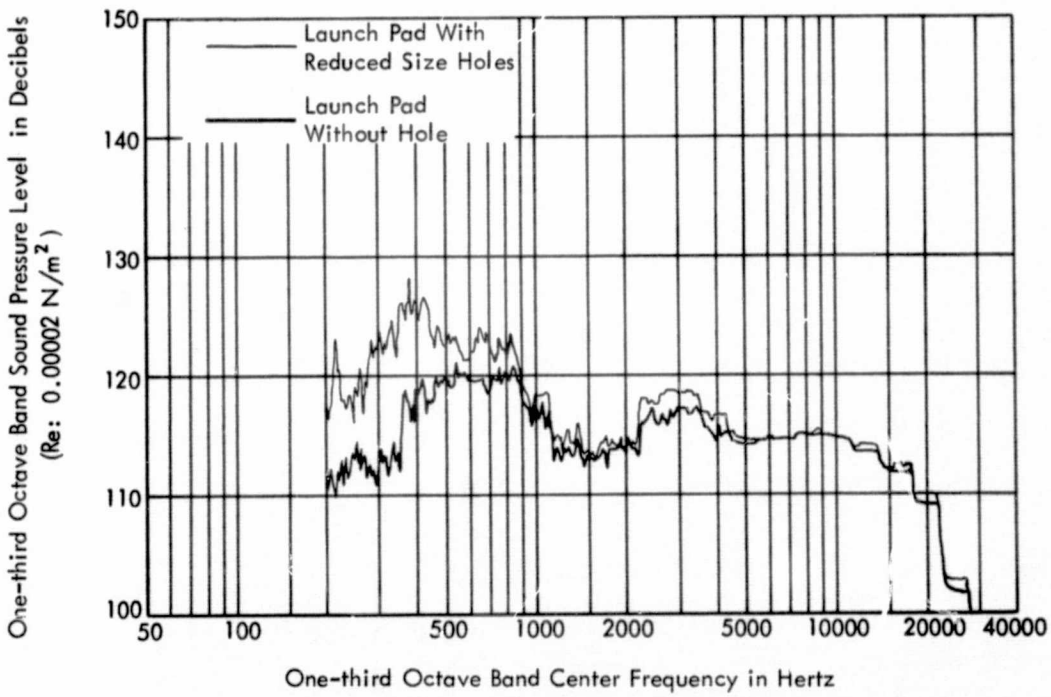

(d) Microphone No. 4

Figure 13. (Continued)

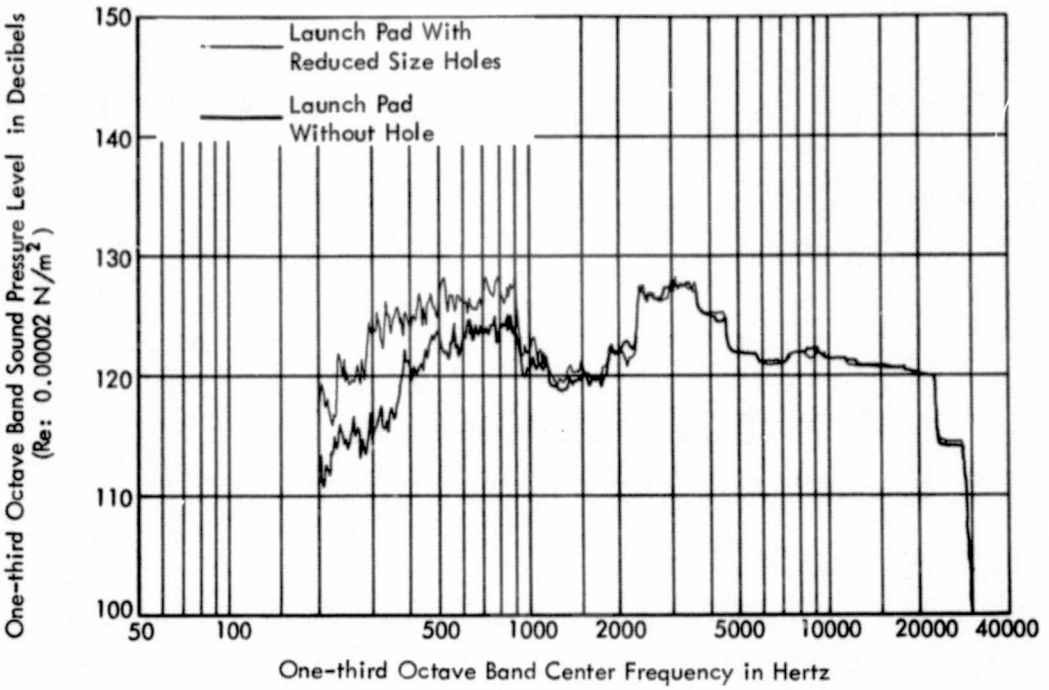

(e) Microphone No. 5

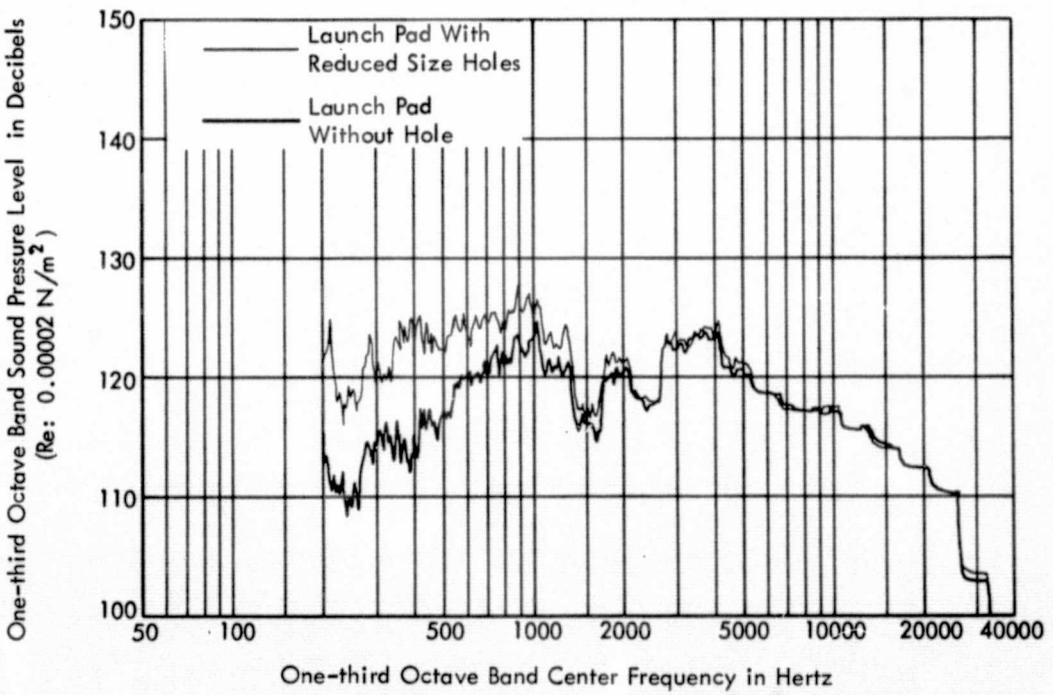

(f) Microphone No. 6

Figure 13. (Continued)

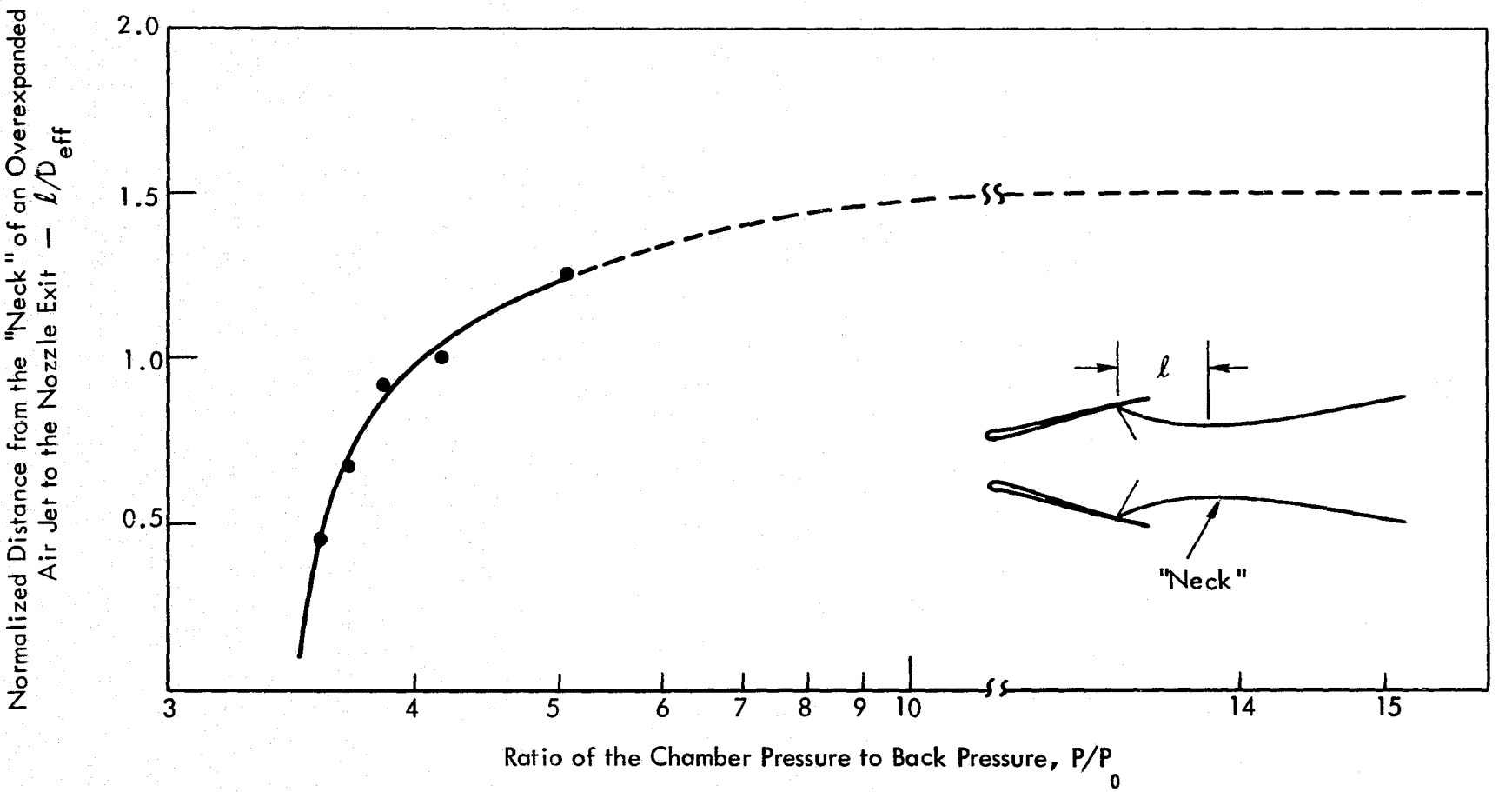

Figure 14. The Normalized Distance from the "Neck" of an Overexpanded Air Jet to the Effective Nozzle Exit Expressed as a Function of the Pressure Ratio of the Jet

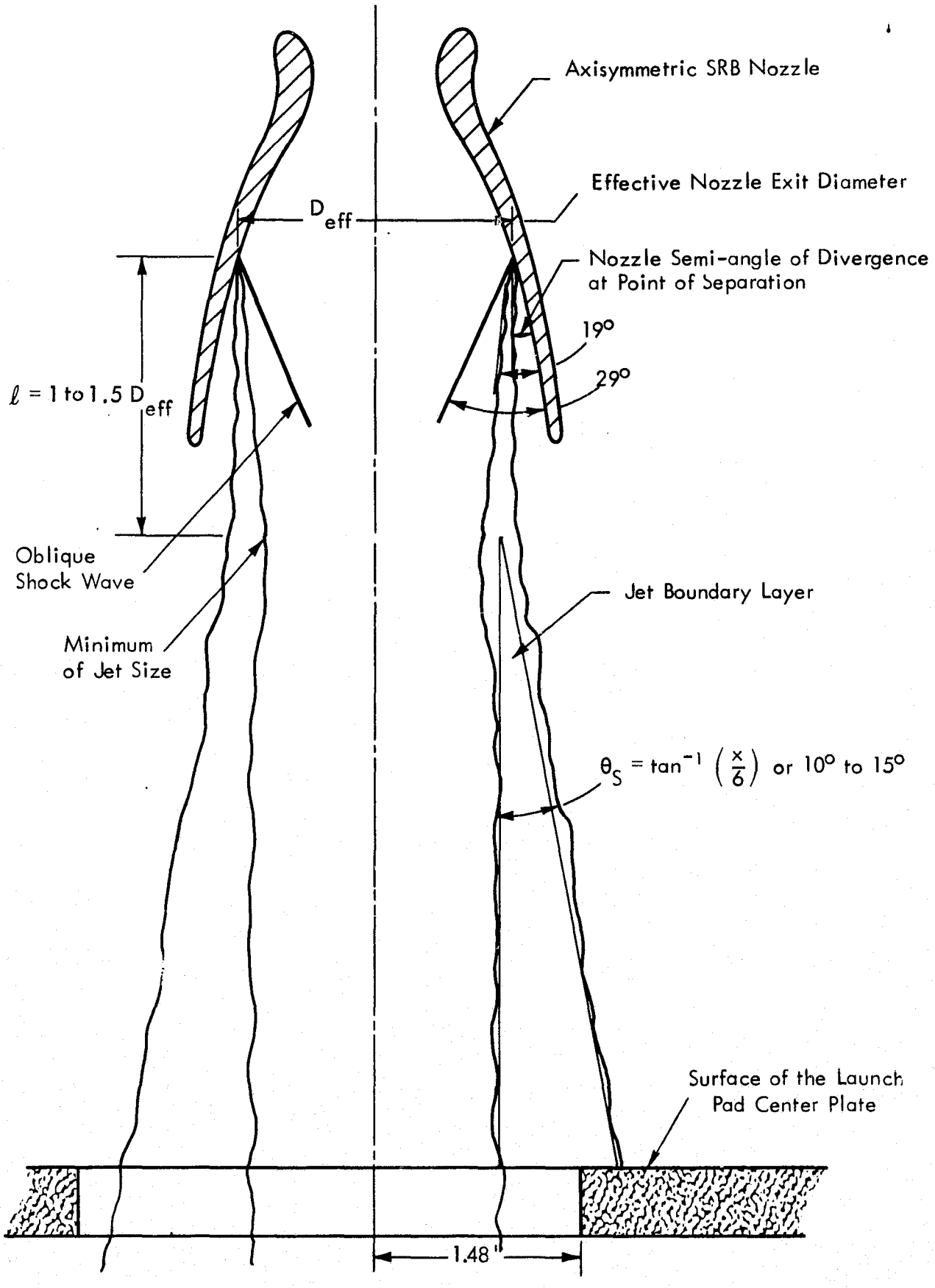

Figure 15. Schematic Diagram of an Idealized, Overexpanded, Supersonic Jet with Flow Separation. (The 1/60 Scale Model SRB Nozzle is Shown Here Full Size.)

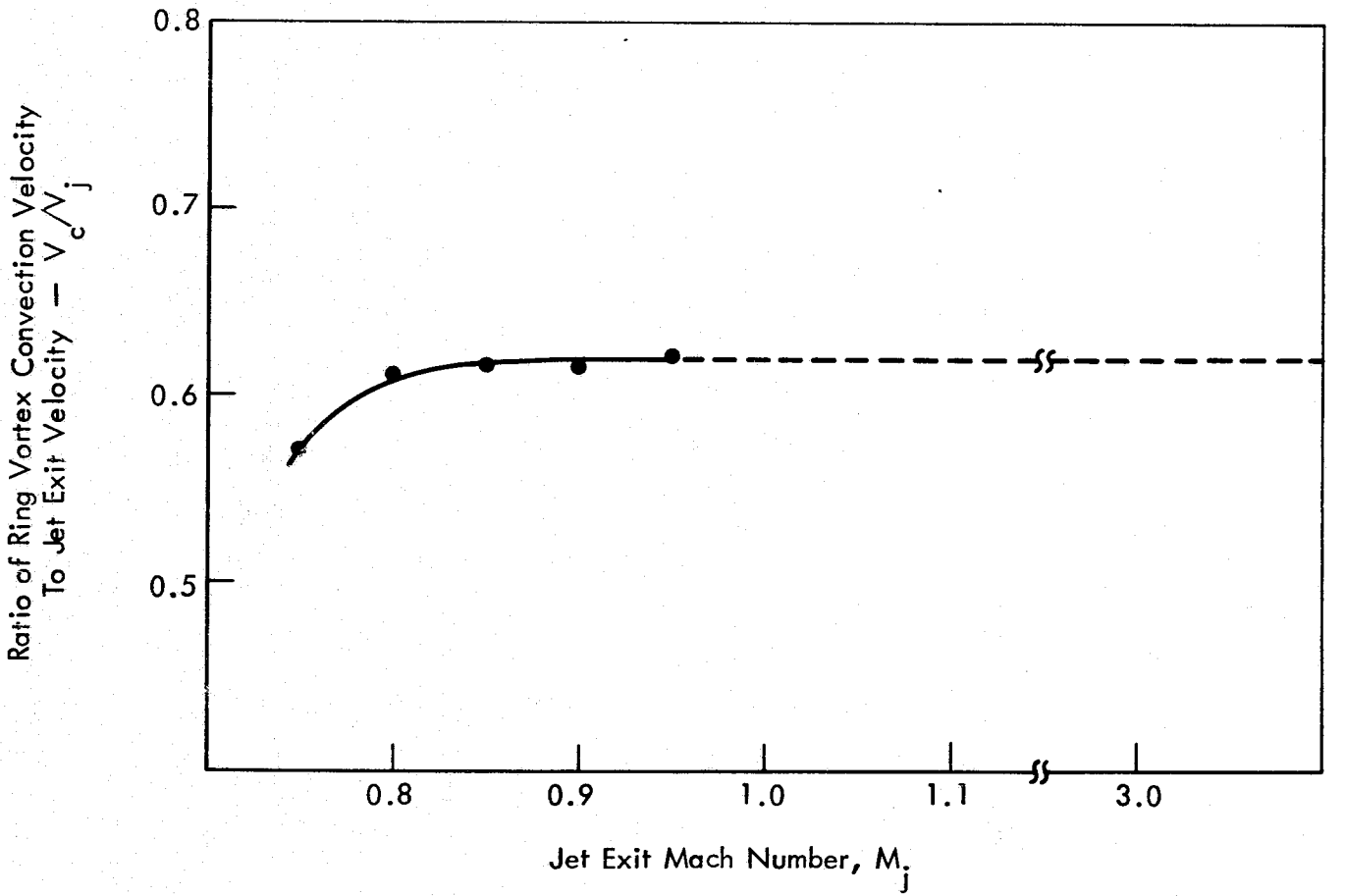

Figure 16. Relationship Between the Normalized Convection Velocity of the Ring Vortex and the Jet Exit Mach Number (Based on Experimental Data of Reference 34)

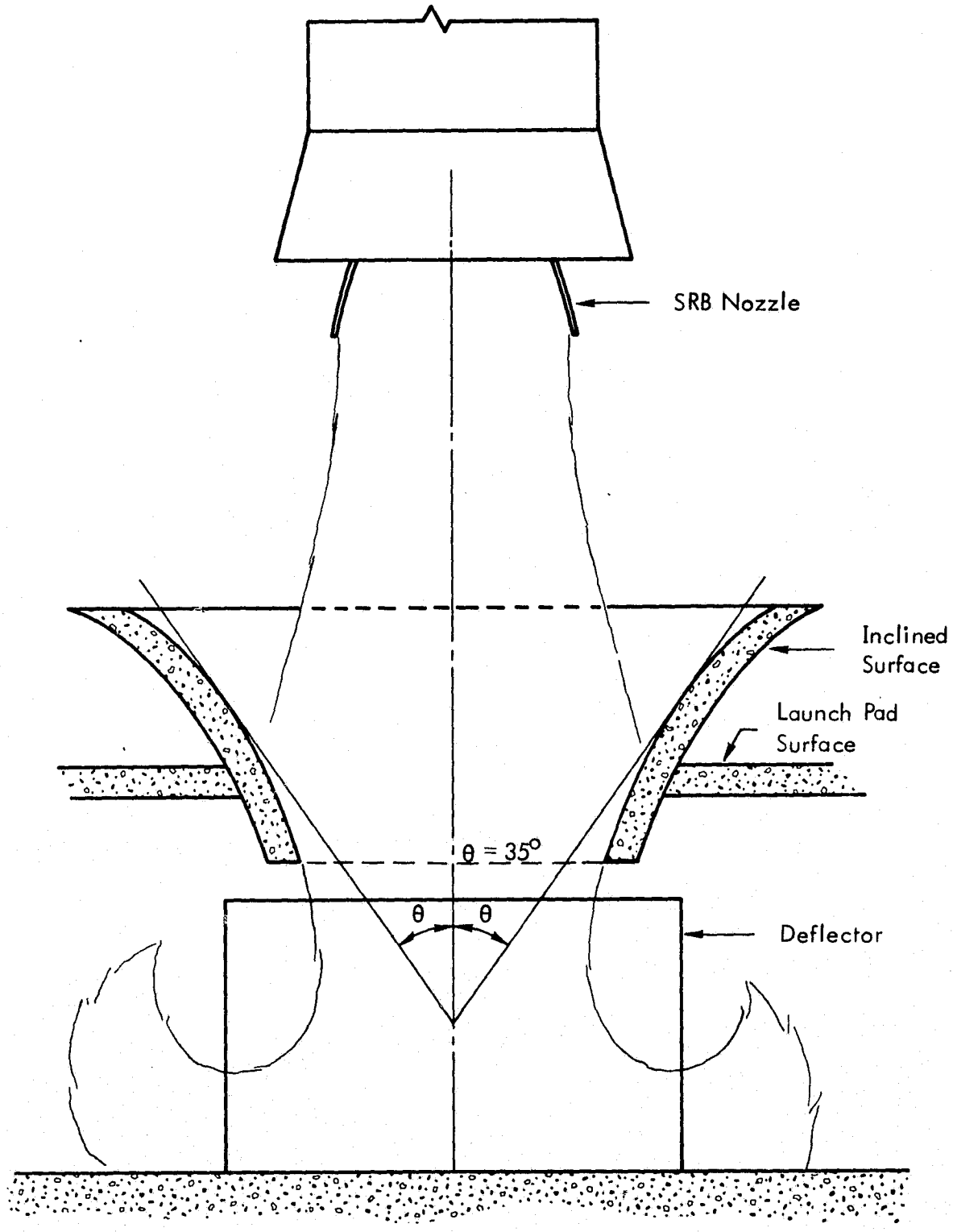

Figure 17. Side View of the Proposed Launch Pad Configuration to Eliminate Screech Noise

APPENDIX A

DETERMINATION OF JET FLOW PARAMETERS

APPENDIX A

DETERMINATION OF JET FLOW PARAMETERS

1.0 PARAMETERS TO BE DETERMINED

In order to use the predictive equations presented in this report for jet screech, the following jet flow parameters must be determined for a separated, over-expanded jet:

- Separation pressure and separation point on the nozzle wall, P_s and L_s
- Nozzle cross-sectional area and diameter in plane of separation A_s and D_s
- Jet exhaust Mach number M_j
- Jet mean flow velocity at the effective nozzle exit, V_j
- Wedge angle, θ_s, by which the jet separates from the nozzle wall
- Angle between nozzle wall and the oblique shock originating from the separation point, θ_w.

2.0 DETERMINATION OF SEPARATION PRESSURE AND SEPARATION POINT ON THE NOZZLE WALL IN AN OVER-EXPANDED ROCKET NOZZLE FLOW

Since the jet flow in the 1/60-scale model test is known to be heavily over-expanded against a back pressure of approximately 14.5 psia, there is no doubt that flow separation takes place. The pressure at which separation occurs and the point of separation from the nozzle wall is determined in the following sections.

2.1 Determination of Separation Pressure

Figure A.1 represents an analysis of the results obtained by different experimenters with rocket motor nozzles having a nozzle divergence half-angle of $\alpha = 15$ degrees. It shows that if $(P_0 - P_s)/P$ is plotted as a function of P/P_0 the results obtained by different experimenters are in substantial agreement [7].

Given that, the tank pressure $P = 218$ psia and back pressure $P_0 = 14.5$ psia; therefore $P/P_0 = 15.0$.

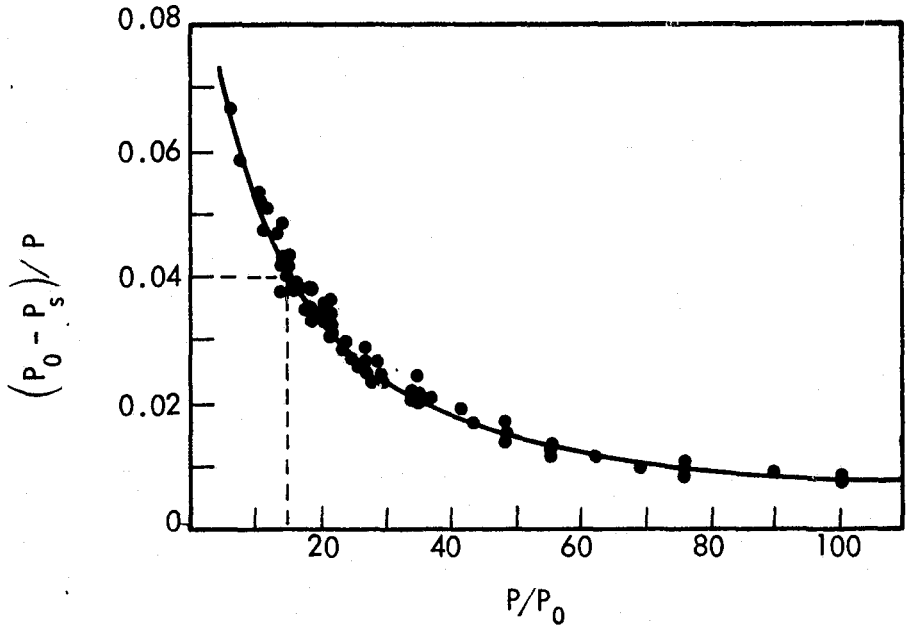

P = Chamber Pressure

P_0 = Back Pressure

P_s = Pressure at Point of Separation

Figure A.1. Data on Flow Separation in Nozzles (Reproduced from Reference 24)

From Figure A.1 it is obtained that

$$(P_0 - P_s) / P \cong 0.04$$

from which $$P_s = P_0 - 0.04\,P = 5.78$$

$$\frac{P_s}{P_0} = 1 - 0.04\,\frac{P}{P_0} = 1 - 0.6 = 0.4$$

$$\therefore \quad \boxed{P_s = 0.4\,P_0}$$

2.2 Determination of Separation Point on the Nozzle Wall

- The nozzle cross-sectional area in the norizontal plane of separation is determined by the following equation available in any text on gas dynamics [6], [48].

$$\frac{A^*}{A} = \frac{\left[1 - \left(P_s/P\right)^{\frac{\gamma-1}{\gamma}}\right]^{\frac{1}{2}} \left(P_s/P\right)^{1/\gamma}}{\left(\frac{\gamma-1}{2}\right)^{\frac{1}{2}} \left(\frac{2}{\gamma-1}\right)^{(\gamma+1)/(\gamma-1)}} \qquad \text{(A-1)}$$

where:

A^* = the cross-section area of nozzle throat when the flow through is at sonic velocity.

A = the nozzle cross-sectional area at the exit.

P_s = separation pressure at point of separation.

P = reservoir tank pressure.

γ = ratio of specific heat of air.

Now, $P = 218$ psia, $\gamma = 1.40$ and, from the previous section, $P_s = 0.4\,P_0 = 5.8$ psia substituted into the above equation. Thus,

$$\frac{A^*}{A} = \frac{A_t}{A_s} = 0.23$$

where A_s is the nozzle cross-sectional area at the separation point.

$$\therefore \quad \frac{A_s}{A_t} = 4.35 \quad \text{and}$$

$$\frac{D_s}{D_t} = \sqrt{4.35} = 2.09$$

Since $D_t = 0.866$ inch

$$\therefore \quad D_s = 1.806 \text{ inch}$$

- The separation point is represented by the axial distance from the nozzle exit to the plane of separation, L_s, and is determined from Figure A.2 by the same method as that in section 2.2 to be:

$$L_s \simeq 1.32 \text{ inch}$$

3.0 DETERMINATION OF THE JET FLOW MACH NUMBER M_j

The Mach number of the jet flow at the effective nozzle exit is determined by:

$$\frac{A}{A^*} = \frac{1}{M_j}\left[\frac{2}{\gamma+1}\left(1+\frac{\gamma-1}{2}M_j^2\right)\right]^{(\gamma+1)/2(\gamma-1)} \qquad \text{(A-2)}$$

For $\gamma = 1.40$ Equation (A-2) becomes 48 :

$$\frac{A}{A^*} = \frac{1}{M_j}\left[\frac{5}{6}\left(1+\frac{M^2}{5}\right)\right]^3$$

From which M_j is computed to be:

$$M_j = 3.01 \quad .$$

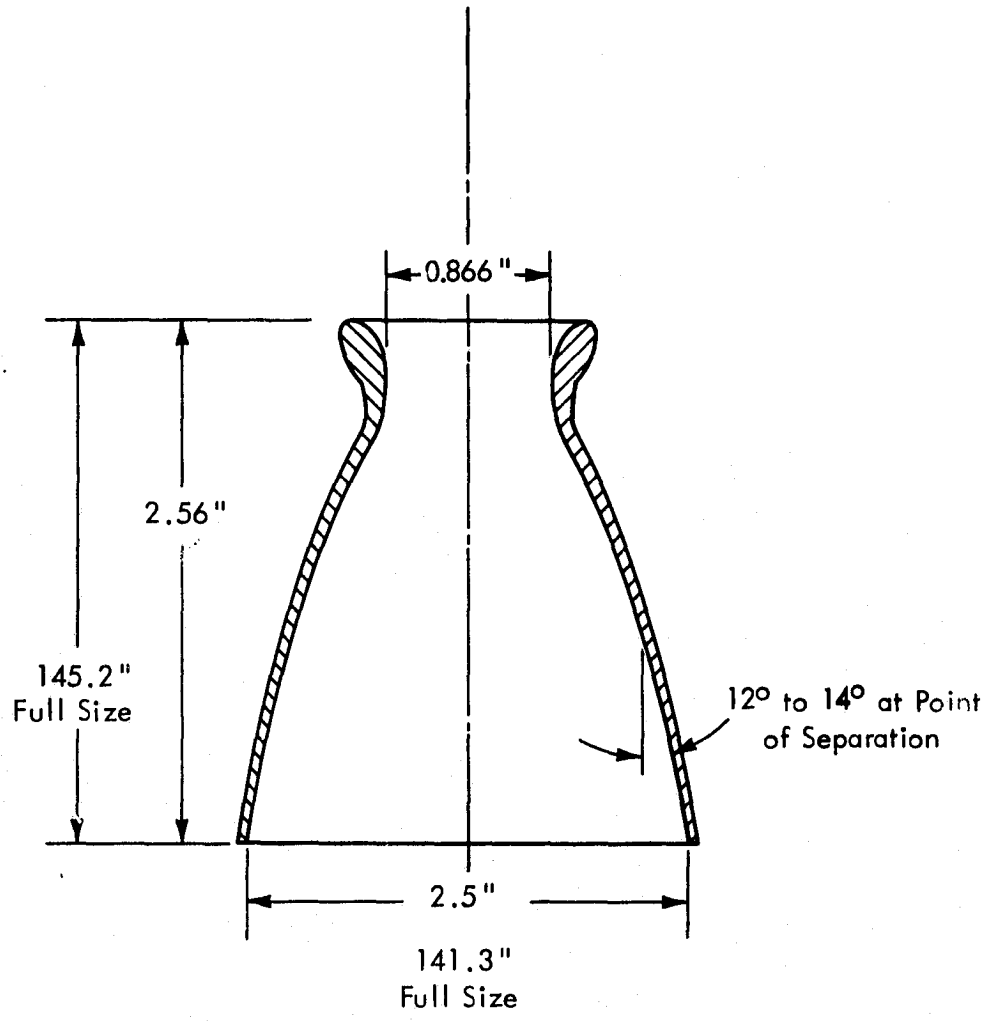

Figure A.2. The 1/60-Scaled Model SRB Nozzle

4.0 JET MEAN FLOW VELOCITY, V_j, AT THE EFFECTIVE NOZZLE EXIT

From reference [48]:

$$\left(\frac{V_j}{a^*}\right) = \frac{6M^2}{5}\left(1 + \frac{M^2}{5}\right)^{-1} \qquad \text{(A-3)}$$

where: a^* = sonic velocity of jet at the nozzle throat in ft/sec

V_j = jet velocity at the effective nozzle exit in ft/sec.

For $M_j = 3.01$ and $a^* = 1110$ ft/sec.

$V_j = 2182.6$ ft/sec = 665 m/sec.

5.0 DETERMINATION OF WEDGE ANGLE, θ_s, AND θ_w, THE ANGLE BETWEEN THE NOZZLE WALL AND THE OBLIQUE SHOCK

The wedge angle, θ_s, by which the jet flow separates from the nozzle wall, as well as the angle between the oblique shock and the nozzle wall, can be determined by a method developed by Mager [31], in which the boundary layer flow inside the nozzle was taken into consideration prior to the determination of θ_s and θ_w. It is of interest to use Mager's method to recalculate the flow parameters obtained in previous sections since Mager's work takes into account the boundary layer flow inside the nozzle and is thus anticipated to provide a more accurate result.

5.1 Separation Pressure P_s

For chamber pressure $P = 218$ psia, and for atmospheric pressure $P_0 = 14.5$ psia

$$\therefore \quad \frac{P_0}{P} = 0.0665$$

From Figure A.3 it is obtained that

$$\frac{P_s}{P} = 0.024$$

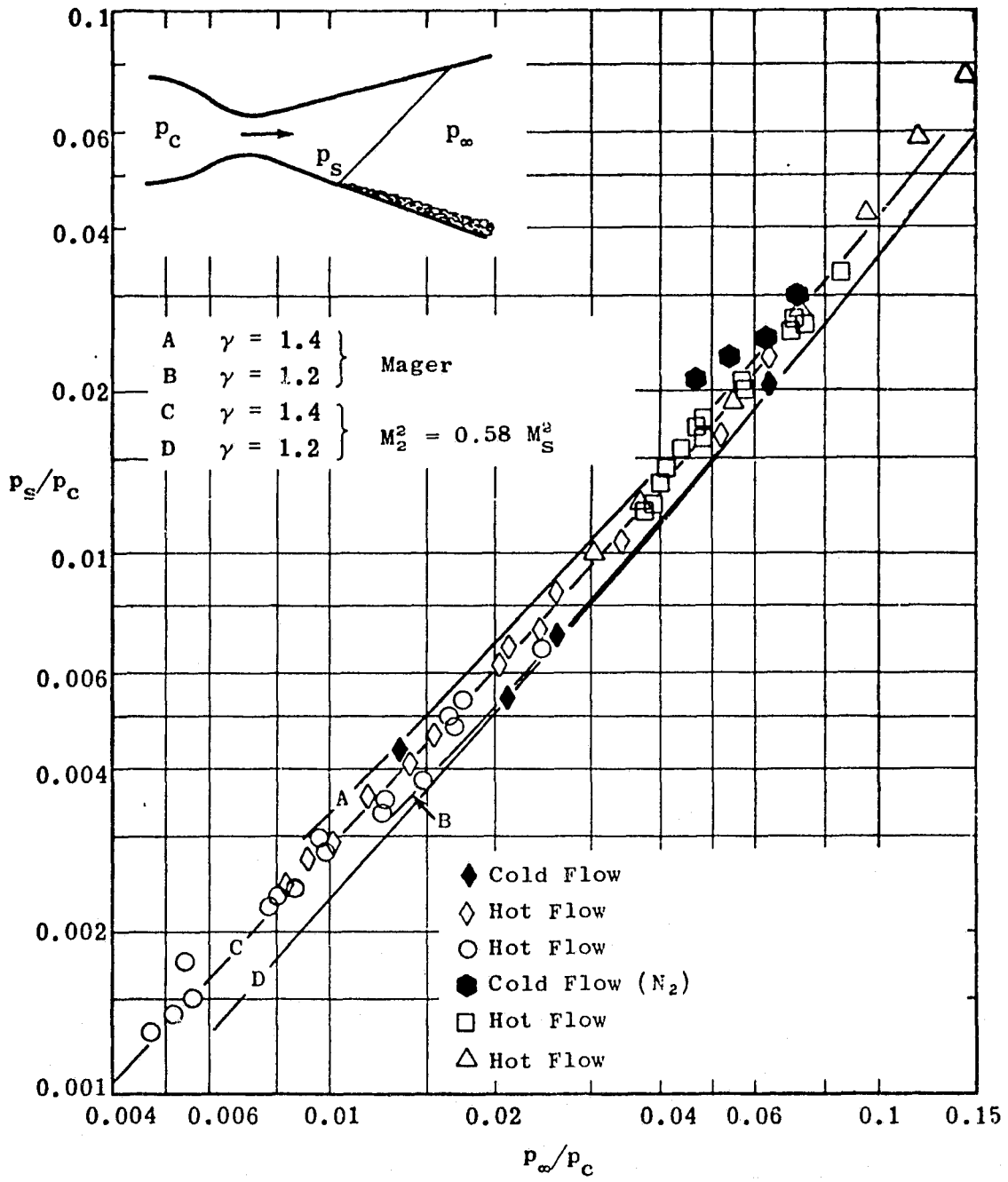

Figure A.3. Comparison of Theoretical and Experimental Values of Separation Pressure Ratio (p_s/p_c) vs Nozzle Pressure Ratio (p_∞/p_c) for Conical Nozzles.

(Reproduced from Reference 31)

$$\therefore \quad P_s = 0.024\, P = 5.232 \text{ psia}$$

$$\text{or} \quad P_s = 0.361\, P_0 \ .$$

5.2 Determination of Separation Point, Jet Mach Number, and Jet Exit Velocity

Substitution of the separation pressure obtained above into Equations (A-1), (A-2), and (A-3) yields:

$$\frac{A_s}{A^*} = \frac{A_s}{A_t} = 4.48 \ ;$$

$$\frac{D_s}{D_t} = 2.12 \ , \longrightarrow \ D_s = 1.835 \text{ inch} \ ;$$

$$M_s = 3.06 \ ;$$

$$V_j = 667 \text{ ft/sec.}$$

The depth of the separation point, L_s, corresponding to $D_s = 1.835$ inch is determined from Figure A.2 to be

$$L_s \simeq 1.3 \text{ inch.}$$

5.3 Determination of θ_s and θ_w

θ_s and θ_w are determined from Figure A.4 for $M_j = 3.06$

$$\theta_s = 19 \text{ degrees}$$

$$\theta_w = 29 \text{ degrees} \ .$$

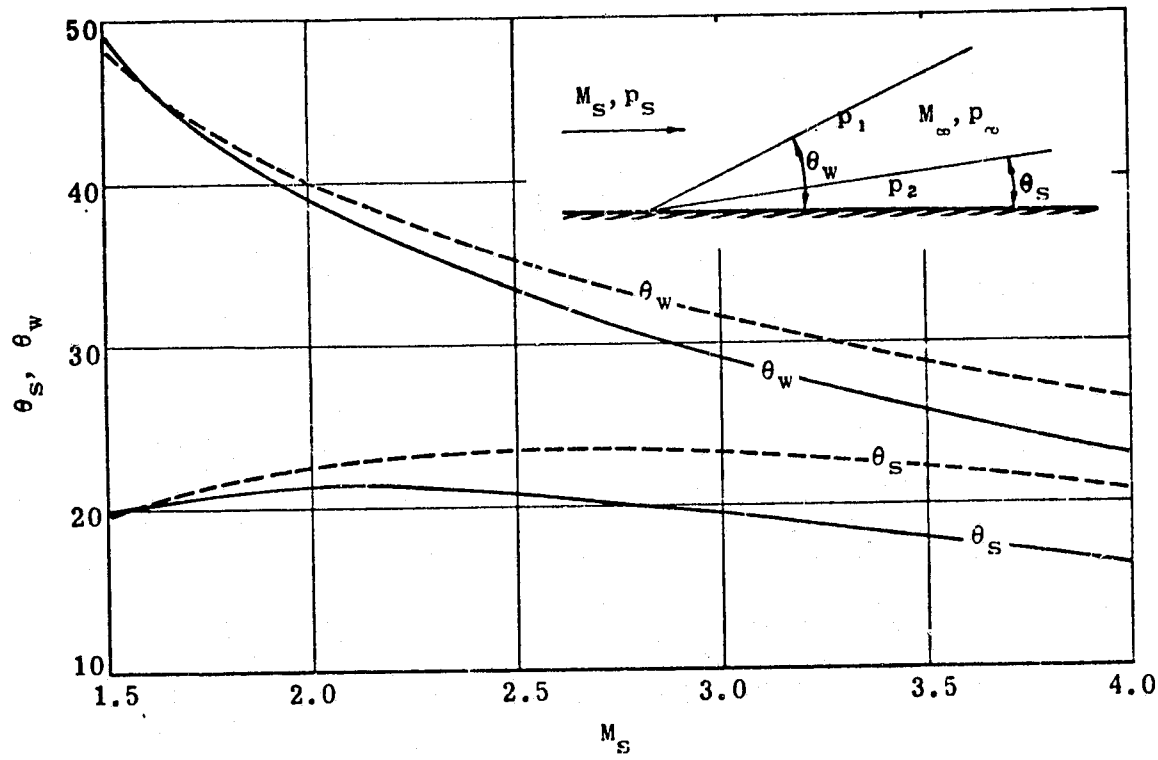

Figure A.4. Pressure Ratios and Related Cone Angles as a Function of Separation Mach Number; Separated Turbulent Boundary Layer in Conical Nozzles; $\gamma = 1.2$ and 1.4.

(Reproduced from Reference 31)

APPENDIX B

DERIVATION OF SCREECH FREQUENCY-PREDICTIVE EQUATION [34]

APPENDIX B

DERIVATION OF SCREECH FREQUENCY-PREDICTIVE EQUATION [34]

Under appropriate conditions the impingement of a jet on an obstructing surface often results in discrete tones due to an acoustic feedback mechanism as previously described in the main report.

In the case of a supersonic jet the shedding of ring vortices is often excited by the pressure disturbances which travels upstream outside the jet in the form of acoustic waves. When the resulting ring vortex is convected downstream and finally strikes the obstructing surface it will give rise to another pressure disturbance which then propagates upstream and excites another ring vortex at the origin of the jet free shear layer. This process continues and the acoustic feedback loop is established.

To maintain the feedback loop, the waves propagating upstream must arrive at the origin of the jet free shear layer at the right moment to excite the shedding of ring vortices. In other words, the frequency of ring vortex shedding must be coincident with the frequency of acoustic wave radiation.

If the frequency of vortex shedding is

$$f_v = \frac{C_v}{\lambda_v} \tag{B-1}$$

and the frequency of acoustic waves is

$$f_w = \frac{C}{\lambda_w} \tag{B-2}$$

where: C_v : the phase velocity of ring vortices

C : speed of sound

λ_v : the wavelength of ring vortex shedding

λ_w : the wavelength of the acoustic wave.

and, if $f_v = f_w$, i.e.

$$f = \frac{C_v}{\lambda_v} = \frac{C}{\lambda_w} \tag{B-3}$$

then, the distance d between the nozzle exit and the obstructing surface must be such that

$$d = m\lambda_v = (n - m)\lambda_w \tag{B-4}$$

where: m : number of vortex periods between the nozzle exit and the obstructing surface

n : total number of periods.

Equation (B-4) yields:

$$\frac{n - m}{n} = \frac{\lambda_v}{\lambda_w}$$

Thus,

$$\frac{n}{m} = 1 + \frac{\lambda_v}{\lambda_w} = 1 + \frac{C_v}{C}$$

or

$$m = \frac{n}{1 + C_v / C} \tag{B-5}$$

Now from Equation (B-1)

$$f = \frac{C_v}{\lambda_v} = \frac{C_v m}{d}$$

Thus,

$$f = \frac{C_v \cdot n}{d\ 1 + C_v / C} \tag{B-6}$$

Equation (B-6) can be further modified in the following form as given in the main report:

$$f = \frac{n \cdot V_j \cdot \left(C_v / V_j\right)}{d\left[1 + \left(C_v / V_j\right)\left(V_j / C\right)\right]}$$

$$= \frac{n V_j \cdot \left(C_v / V_j\right)}{d\left[1 + \left(C_v / V_j\right) M_j\right]}$$

where $\frac{C_v}{V_j}$ is known from experiments to be approximately a constant for a given jet.